

Supporting Information

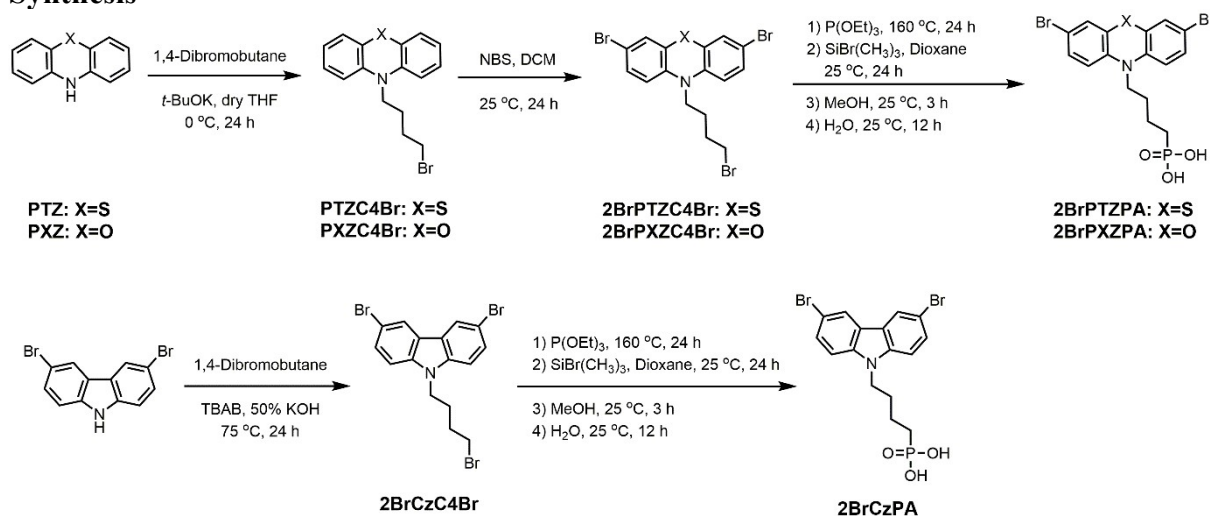
Simple and Robust Phenoxazine Phosphonic Acid Molecules as Self-assembled Hole selective contacts for High-performance Inverted Perovskite Solar Cells

Zhaoning Li[‡], Qin Tan[‡], Guocong Chen, Han Gao, Jiafeng Wang, Xusheng Zhang, Jingwei Xiu, Wei Chen, Zhubing He*

Department of Materials Science and Engineering, Institute of Innovative Materials (I2M), Shenzhen Key Laboratory of Full Spectral Solar Electricity Generation (FSSEG), Southern University of Science and Technology, No. 1088, Xueyuan Rd., Shenzhen, 518055, Guangdong, China. Z.L. and Q.T. contributed equally to this work.

Corresponding email: hezb@sustech.edu.cn

Synthesis



Scheme 1 Synthetic route of 2BrPXZPA, 2BrPTZPA and 2BrCzPA.

Synthesis of 10-(4-bromobutyl)-10H-phenothiazine (PTZC4Br)

A 100 mL two neck flask was charged with 10H-phenothiazine (4.00 g, 20.0 mmol) and potassium tert-butoxide (13.40 g, 120 mmol) dissolved in anhydrous THF (40 mL) and stirred for 1 h in ice bath. Then, 1,4-Dibromobutane (25.90 g, 120.0 mmol) in anhydrous THF (20 mL) was added dropwise. The mixture was warmed up to the room temperature and stirred overnight. The reaction was quenched with water and extracted with dichloromethane, the organic layers were combined and dried with anhydrous magnesium sulfate, then removed the

organic solvent with rotary evaporator to get the crude product. Silica gel column chromatography was used for further purification with eluant as petroleum ether/dichloromethane = 10/1 to give the title compound as light yellow oil (3.00 g, yield 45%).

¹H NMR (400 MHz, Chloroform-d) δ 7.20 – 7.14 (m, 4H), 6.94 (td, J = 7.5, 1.2 Hz, 2H), 6.88 (dd, J = 8.5, 1.2 Hz, 2H), 3.97 – 3.83 (m, 2H), 3.49 – 3.32 (m, 2H), 1.99 (tt, J = 6.0, 3.0 Hz, 4H) ppm.

¹³C NMR (101 MHz, Chloroform-d) δ 145.17, 127.62, 127.29, 125.51, 122.63, 115.57, 46.19, 33.53, 29.93, 25.31 ppm.

Synthesis of 10-(4-bromobutyl)-10H-phenoxazine (PXZC4Br)

The PXZC4Br was synthesized in the same way as PTZC4Br to give the title compound as white solid (2.20 g, yield 55%).

¹H NMR (400 MHz, Chloroform-d) δ 6.81 (ddd, J = 8.0, 6.3, 2.7 Hz, 2H), 6.72 – 6.61 (m, 4H), 6.49 (d, J = 8.6 Hz, 2H), 3.54 (t, J = 7.8 Hz, 2H), 3.48 (t, J = 6.6 Hz, 2H), 2.06 – 1.95 (m, 2H), 1.90 – 1.79 (m, 2H) ppm.

¹³C NMR (101 MHz, Chloroform-d) δ 145.04, 133.20, 123.69, 120.97, 115.50, 111.29, 43.14, 33.02, 29.97, 23.78 ppm.

Synthesis of 3,7-dibromo-10-(4-bromobutyl)-10H-phenothiazine (2BrPTZC4Br)

A 100 mL round bottom flask was charged with PTZC4Br (1.35 g, 4.24 mmol) and dichloromethane (20 mL) in ice bath, then N-Bromosuccinimide (1.51 g, 8.48 mmol) was added in portion. The mixture was warmed up to room temperature and stirred overnight. The reaction was quenched with water and extracted with dichloromethane, the organic layers were combined and dried with anhydrous magnesium sulfate, then removed the organic solvent with rotary evaporator to give the crude product. A flash column chromatography with eluent as petroleum ether/dichloromethane of 20/1 to 5/1 was used to further purification. The title compound was colorless oil (1.72 g, yield 83%).

¹H NMR (400 MHz, Chloroform-d) δ 7.30 – 7.18 (m, 4H), 6.69 (d, J = 8.5 Hz, 2H), 3.82 (t, J = 6.2 Hz, 2H), 3.39 (t, J = 6.2 Hz, 2H), 2.04 – 1.81 (m, 4H) ppm.

¹³C NMR (101 MHz, Chloroform-d) δ 143.96, 130.25, 129.91, 126.98, 116.81, 115.11, 46.45, 33.25, 29.68, 25.06 ppm.

Synthesis of 3,7-dibromo-10-(4-bromobutyl)-10H-phenoxazine (2BrPXZC4Br)

The 2BrPXZC4Br was synthesized in the same way as 2BrPTZC4Br to give the title compound as white solid (3.67 g, yield 87%).

¹H NMR (400 MHz, Chloroform-d) δ 6.91 (dt, J = 8.6, 2.2 Hz, 2H), 6.78 – 6.70 (m, 2H), 6.32 (dd, J = 8.5, 3.3 Hz, 2H), 3.47 (t, J = 6.4 Hz, 4H), 2.06 – 1.90 (m, 2H), 1.86 – 1.72 (m, 2H) ppm.

¹³C NMR (101 MHz, Chloroform-d) δ 145.22, 141.60, 131.96, 126.63, 118.76, 112.53, 112.44, 43.32, 32.83, 32.81, 29.69, 23.43 ppm.

Synthesis of (4-(3,7-dibromo-10H-phenothiazin-10-yl)butyl)phosphonic acid (2BrPTZPA)

A 100 mL Schlenk tube was charged with 2BrPTZC4Br (2.50 g, 5.08 mmol) and triethyl phosphite (20 mL), then the mixture was heated to 160°C and stirred overnight under nitrogen atmosphere. The extra triethyl phosphite was removed by reduced pressure distillation to give a light-yellow oil without further purification. The oil was dissolved in anhydrous 1,4-dioxane (20 mL) at room temperature and trimethylbromosilane (7.78 g, 50.8 mmol) was added dropwise, then the mixture was stirred overnight. The 1,4-dioxane was removed with rotary evaporator to give a white solid. The white solid was dissolved in methanol (20 mL) at room temperature, then deionized water was added dropwise until the mixture became opaque and stirred for another 12 h. The crude product was collected by filtration and washed with deionized water. The crude product was dissolved in THF (5 mL) and reprecipitate in acetone (20 mL) and filtrated to give the final product as baby blue solid (1.50 g, yield 60%).

¹H NMR (500 MHz, DMSO-d₆) δ 7.38 – 7.32 (m, 4H), 6.99 – 6.96 (m, 2H), 3.82 (t, J = 7.0 Hz, 2H), 1.72 (t, J = 7.1 Hz, 2H), 1.64 – 1.44 (m, 4H) ppm.

¹³C NMR (126 MHz, DMSO-d₆) δ 144.24, 130.84, 129.53, 125.84, 118.10, 114.51, 46.85, 28.06, 27.39, 27.26, 26.97, 20.63, 20.60 ppm.

³¹P NMR (202 MHz, DMSO-d₆) δ 26.45 ppm.

Anal. calcd for C₁₆H₁₆Br₂NO₃PS, %: C 38.97, H 3.27, N 2.84, found, %: C 39.12, H 3.25, N 2.52.

HRMS m/z calcd for C₁₆H₁₆Br₂NO₃PS [M+H]⁺ 493.9008, found 493.8997.

Synthesis of (4-(3,7-dibromo-10H-phenoxazin-10-yl)butyl)phosphonic acid (2BrPXZPA)

The 2BrPXZPA was synthesized in the same way as 2BrPTZPA to give the final compound as blue solid (1.33 g, yield 65%).

¹H NMR (500 MHz, DMSO-d₆) δ 7.00 (dd, J = 8.6, 2.3 Hz, 2H), 6.83 (d, J = 2.3 Hz, 2H), 6.68 (d, J = 8.7 Hz, 2H), 3.51 (t, J = 6.9 Hz, 2H), 1.59 (m, 6H) ppm.

¹³C NMR (126 MHz, DMSO-d₆) δ 144.94, 132.38, 127.39, 118.21, 114.31, 111.81, 43.26, 28.19, 27.10, 25.36, 25.24, 20.42, 20.38 ppm.

³¹P NMR (202 MHz, DMSO-d₆) δ 26.28 ppm.

Anal. calcd for $C_{16}H_{16}Br_2NO_4P$, %: C 40.28, H 3.38, N 2.94, found, %: C 40.30, H 3.40, N 2.72.

HRMS m/z calcd for $C_{16}H_{16}Br_2NO_4P$ [$M+H$]⁺ 477.9236, found 477.9230.

Synthesis of 3,6-dibromo-9-(4-bromobutyl)-9H-carbazole (2BrCzC4Br)

A 100 mL round bottom flask was charged with 3,6-dibromo-9H-carbazole (1.00 g, 3.08 mmol), tetrabutylammonium bromide (0.10 g, 0.31 mmol) and 1,4-dibromobutane (20 mL). 50% potassium hydroxide aqueous solution was added slowly, and the mixture was heated to 70°C for overnight. The reaction was quenched by water and extracted with dichloromethane, the organic layers were combined and dried with anhydrous magnesium sulfate and concentrated by rotary evaporator. The crude product was further purification by silica gel chromatography with eluent as petroleum ether/dichloromethane = 5/1 to give the title compound as white powder (1.18 g, yield 83%).

¹H NMR (500 MHz, Chloroform-d) δ 8.16 (d, J = 1.9 Hz, 2H), 7.58 (dd, J = 8.7, 2.0 Hz, 2H), 7.29 (d, J = 8.7 Hz, 2H), 4.31 (t, J = 7.1 Hz, 2H), 3.40 (t, J = 6.5 Hz, 2H), 2.05 (dt, J = 9.6, 6.8 Hz, 2H), 1.89 (dt, J = 17.1, 6.7 Hz, 2H) ppm.

¹³C NMR (101 MHz, Chloroform-d) δ 139.17, 129.19, 123.54, 123.38, 112.21, 110.27, 42.47, 32.86, 30.04, 27.47 ppm.

Synthesis of 4-(3,6-dibromo-9H-carbazol-9-yl)butylphosphonic acid (2BrCzPA)

The 2BrCzPA was synthesized in the same way as 2BrPTZPA and 2BrPXZPA to give the final product as white solid (0.94 g, yield 80%).

¹H NMR (500 MHz, DMSO-d₆) δ 8.47 (s, 2H), 7.64 (d, J = 8.8 Hz, 2H), 7.59 (dd, J = 8.7, 2.0 Hz, 2H), 4.39 (t, J = 7.1 Hz, 2H), 1.81 (q, J = 7.3 Hz, 2H), 1.60 – 1.40 (m, 4H) ppm.

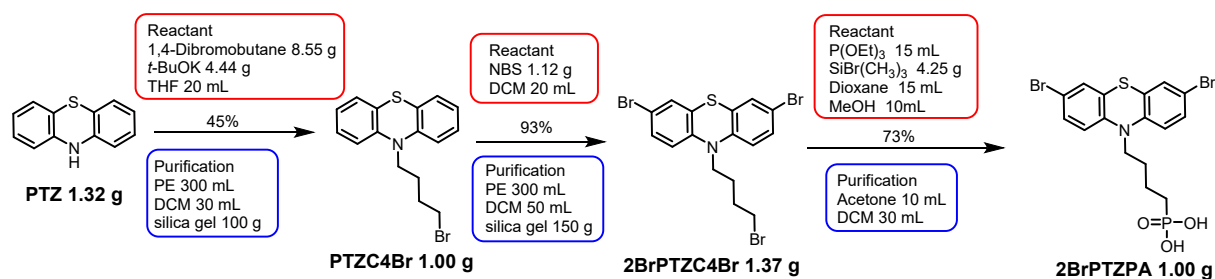
¹³C NMR (126 MHz, DMSO-d₆) δ 139.50, 129.28, 123.88, 123.36, 112.22, 111.72, 42.75, 29.93, 29.81, 28.25, 27.16, 20.80, 20.76 ppm.

³¹P NMR (202 MHz, DMSO) δ 26.36 ppm.

Anal. calcd for $C_{16}H_{16}Br_2NO_3P$, %: C 41.68, H 3.50, N 3.04, found, %: C 41.81, H 3.48, N 2.84.

HRMS m/z calcd for $C_{16}H_{16}Br_2NO_3P$ [$M+H$]⁺ 461.9287, found 461.9275.

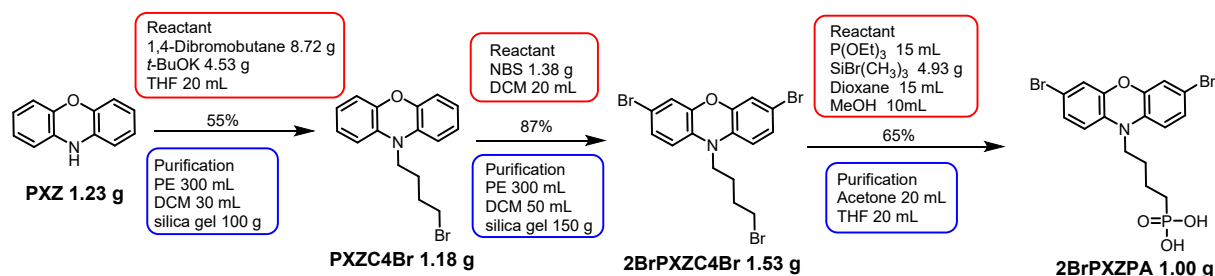
Synthetic cost analysis



Scheme S2 Dosage of chemical reagents in reaction (red box) and purification (blue box) for 1 g 2BrPTZPA.

Table S1 The detailed cost calculation of chemical reagent for 1 g 2BrPTZPA

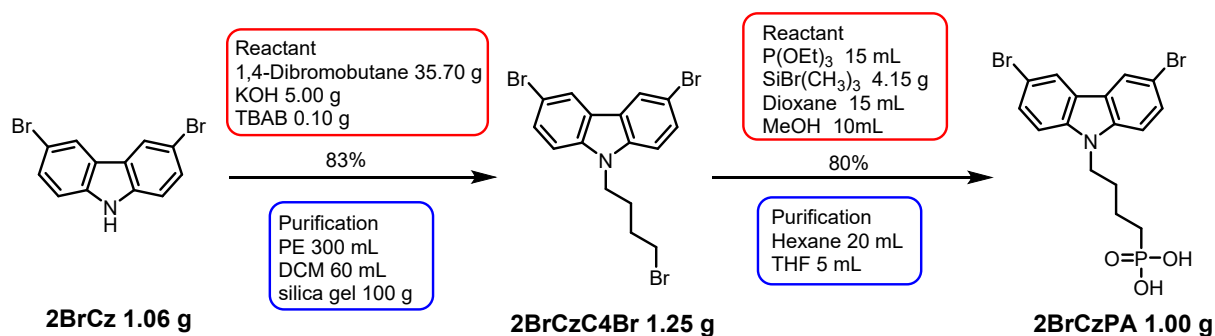
| Chemicals | Price (RMB) | Dosage | Cost (RMB) |
|-------------------------------------|--------------|--------|------------------------|
| Phenothiazine | 25 g/22.8 | 1.32 g | 1.204 |
| 1,4-Dibromobutane | 500 g/112.48 | 8.55 g | 1.923 |
| <i>t</i> -BuOK | 100 g/82.4 | 4.44 g | 3.658 |
| NBS | 100 g/28.5 | 1.12 g | 0.319 |
| P(OEt) ₃ | 500 mL/79.5 | 15 mL | 2.385 |
| SiBr(CH ₃) ₃ | 100 g/106 | 4.25 g | 4.505 |
| THF | 500 mL/66 | 20 mL | 2.640 |
| Dioxane | 500 mL/208.8 | 15 mL | 6.255 |
| DCM | 5L/110 | 130 mL | 2.860 |
| PE | 5L/79 | 600 mL | 9.480 |
| Acetone | 500 mL/25 | 10 mL | 0.500 |
| Silica gel | 1000 g/60 | 250 g | 15.000 |
| Total | | | 50.73 (7.96 \$) |



Scheme S3 Dosage of chemical reagents in reaction (red box) and purification (blue box) for 1 g 2BrPXZPA.

Table S2 The detailed cost calculation of chemical reagent for 1 g 2BrPXZPA

| Chemicals | Price (RMB) | Dosage | Cost (RMB) |
|-------------------------------------|--------------|--------|-------------------------|
| Phenoxazine | 5 g/186.96 | 1.23 g | 45.992 |
| 1,4-Dibromobutane | 500 g/112.48 | 8.72 g | 1.962 |
| <i>t</i> -BuOK | 100 g/82.4 | 4.53 g | 3.733 |
| NBS | 100 g/28.5 | 1.38 g | 0.393 |
| P(OEt) ₃ | 500 mL/79.5 | 15 mL | 2.385 |
| SiBr(CH ₃) ₃ | 100 g/106 | 4.93 g | 5.226 |
| THF | 500 mL/66 | 40 mL | 5.280 |
| Dioxane | 500 mL/208.8 | 15 mL | 6.255 |
| DCM | 5L/110 | 100 mL | 2.200 |
| PE | 5L/79 | 600 mL | 9.480 |
| Acetone | 500 mL/25 | 20 mL | 1.000 |
| Silica gel | 1000 g/60 | 250 g | 15.000 |
| Total | | | 98.91 (15.51 \$) |



Scheme S4 Dosage of chemical reagents in reaction (red box) and purification (blue box) for 1 g 2BrCzPA.

Table S3 The detailed cost calculation of chemical reagent for 1 g 2BrCzPA

| Chemicals | Price (RMB) | Dosage | Cost (RMB) |
|-------------------------------------|--------------|--------|------------|
| 3,6-Dibromocarbazole | 25 g/112.5 | 1.06 g | 4.770 |
| 1,4-Dibromobutane | 500 g/112.48 | 35.7 g | 8.030 |
| KOH | 500 g/15 | 5.00 g | 0.150 |
| TBAB | 100 g/19 | 0.1 g | 0.019 |
| P(OEt) ₃ | 500 mL/79.5 | 15 mL | 2.385 |
| SiBr(CH ₃) ₃ | 100 g/106 | 4.15 g | 4.399 |
| THF | 500 mL/66 | 5 mL | 0.660 |
| Dioxane | 500 mL/208.8 | 15 mL | 6.255 |

| | | | |
|-------------------|-----------|--------|-----------------|
| DCM | 5L/110 | 60 mL | 1.320 |
| PE | 5L/79 | 300 mL | 4.74 |
| Hexane | 500 mL/18 | 20 mL | 0.720 |
| Silica gel | 1000 g/60 | 100 g | 6.000 |
| Total | | | 39.45 (6.18 \$) |

PACz series molecules

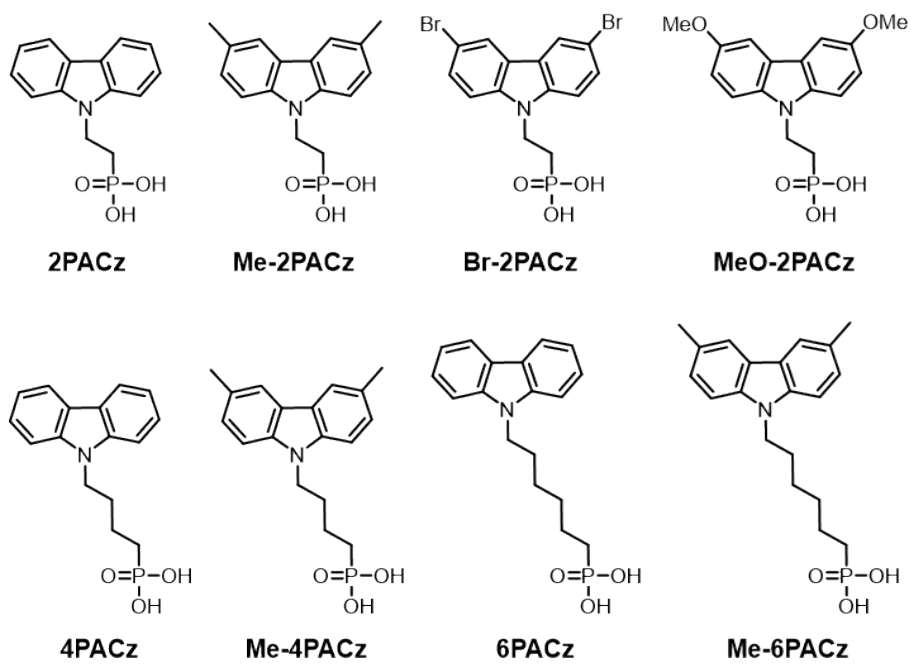


Figure S1 The chemical structures of PACz series molecules.

DFT calculation

The DFT calculations were performed with the Gaussian 09 revision D.01 suite [1]. Initially the ground state geometry was optimized using a DFT methodology employing the B3LYP functional with the 6-311G* basis set. Time-dependent DFT (TD-DFT) was used to simulate the excited state and absorption spectra with the same method and basis set. The molecular orbitals were visualized using the GaussView 5.0 software. The dipole moment calculation was followed the reported method [2] with B3LYP functional and def2-SVP basis set, and the phosphonic acid group was replaced with hydrogen.

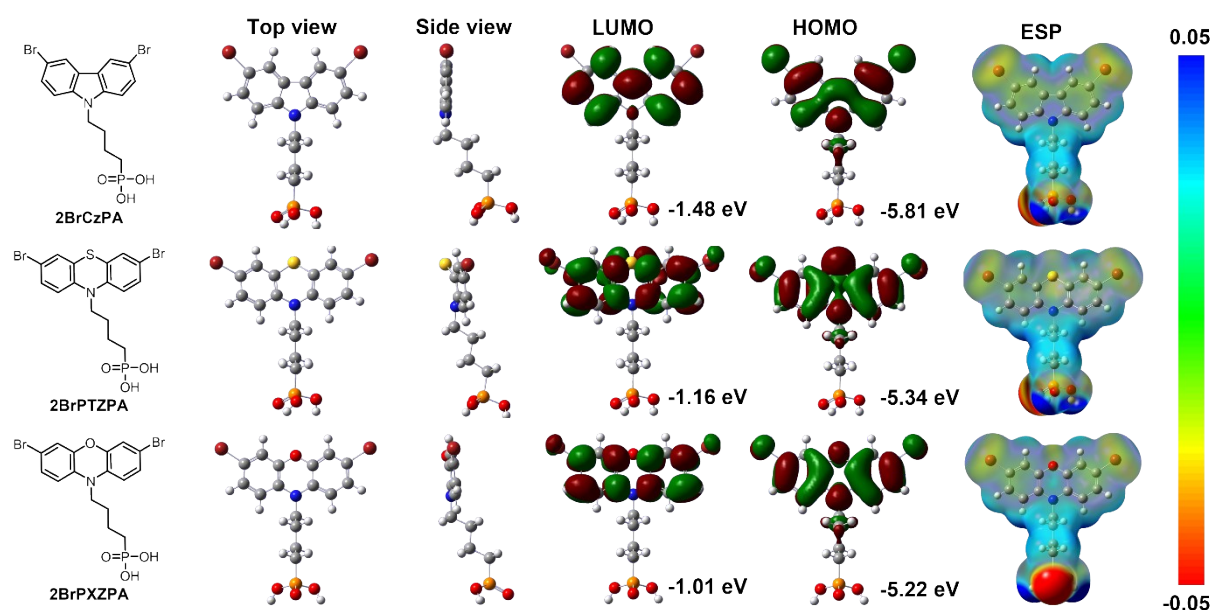


Figure S2 DFT calculation results of 2BrCzPA, 2BrPTZPA and 2BrPXZPA. The optimized molecular geometry, corresponding HOMO and LUMO orbitals and electrostatic surface potential (ESP) were simulated with B3LYP/6-311G*.

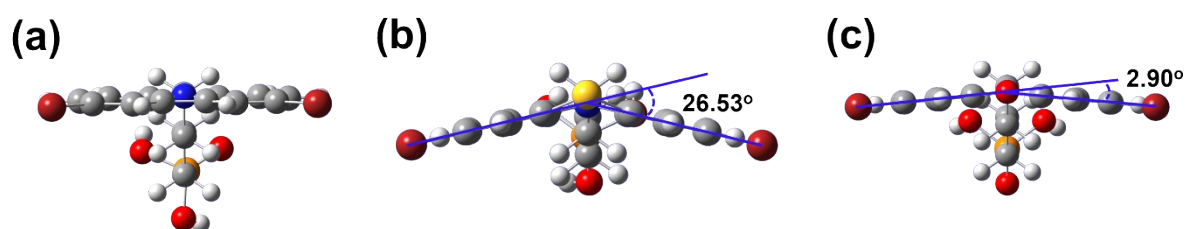


Figure S3 Intramolecular dihedral angle of (a) 2BrCzPA, (b) 2BrPTZPA and (c) 2BrPXZPA evaluate from the optimized chemical structure with B3LYP/def2-SVP (C: gray, H: white, O: red, N: blue, S: yellow, Br: dark red).

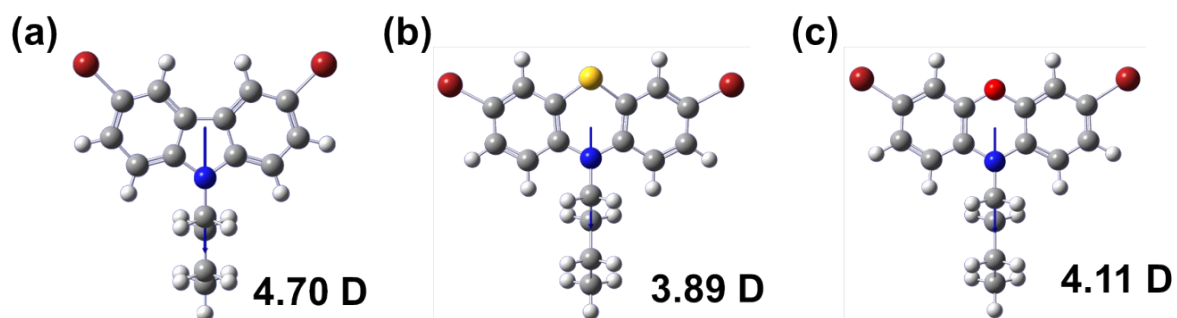


Figure S4 Electronic dipole moment of (a) 2BrCzPA, (b) 2BrPTZPA and (c) 2BrPXZPA with direction of σ^+ to σ^- .

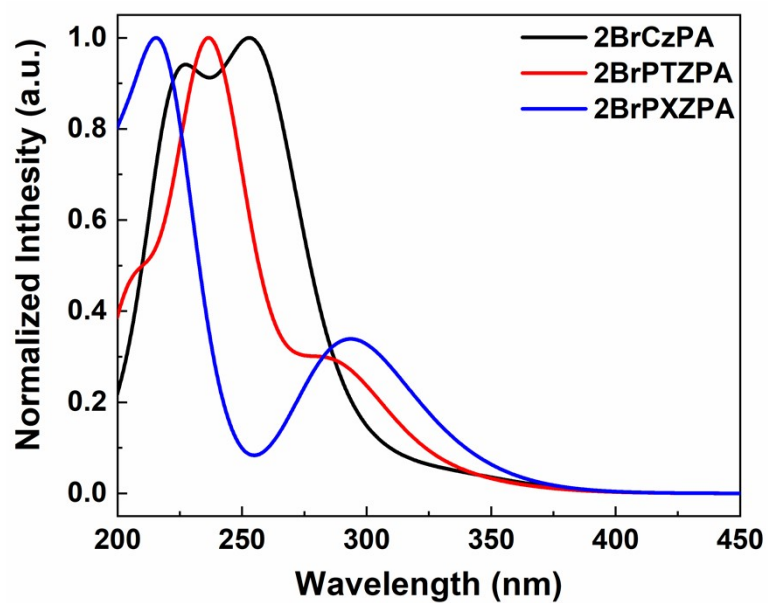


Figure S5 Simulated UV-vis absorption spectra of 2BrCzPA, 2BrPTZPA and 2BrPXZPA based on TD-DFT with B3LYP/6-311G*.

TGA

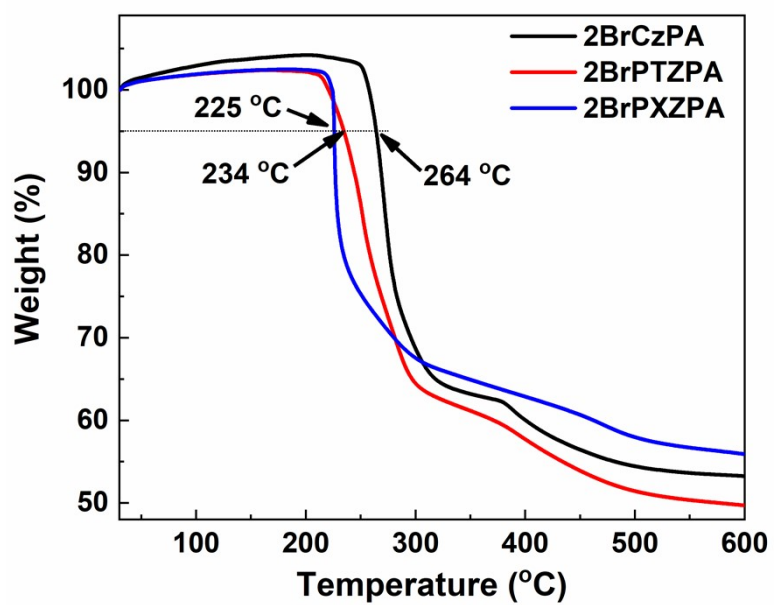


Figure S6 TGA of 2BrCzC4PA, 2BrPXZPA and 2BrPTZPA with a heating rate of 10 °C/min in nitrogen flow.

Kelvin Probe Force Microscope (KPFM)

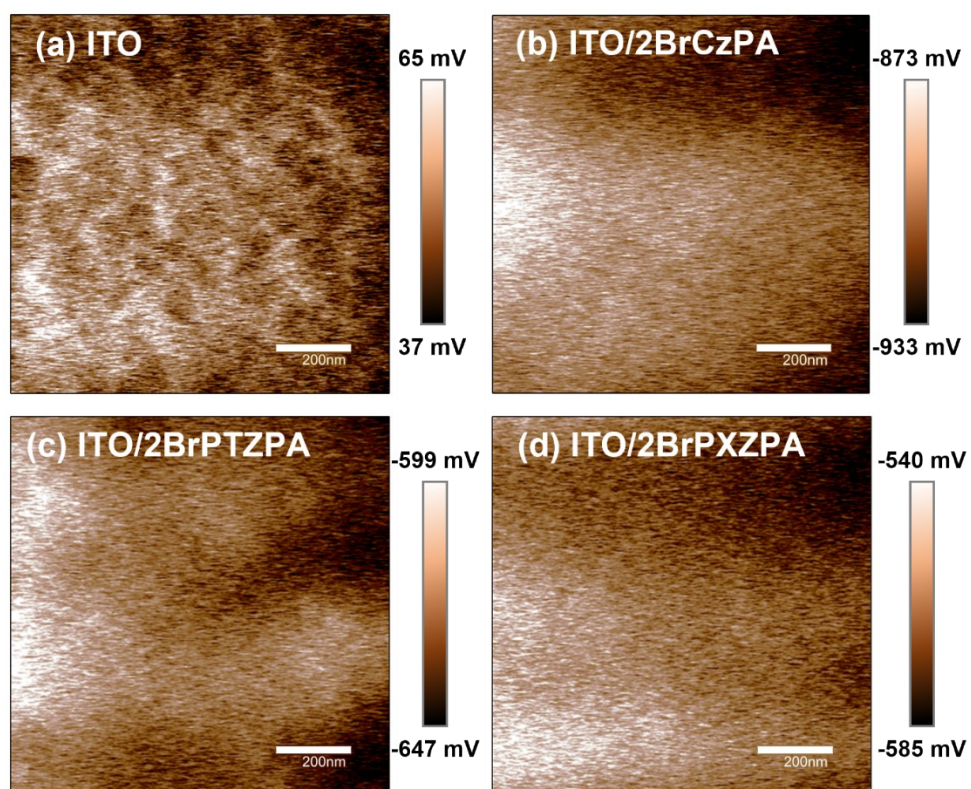


Figure S7 KPFM of (a) bare ITO and ITO with (b) 2BrCzPA, (c) 2BrPTZPA and (d) 2BrPXZPA modification.

Band bending diagram

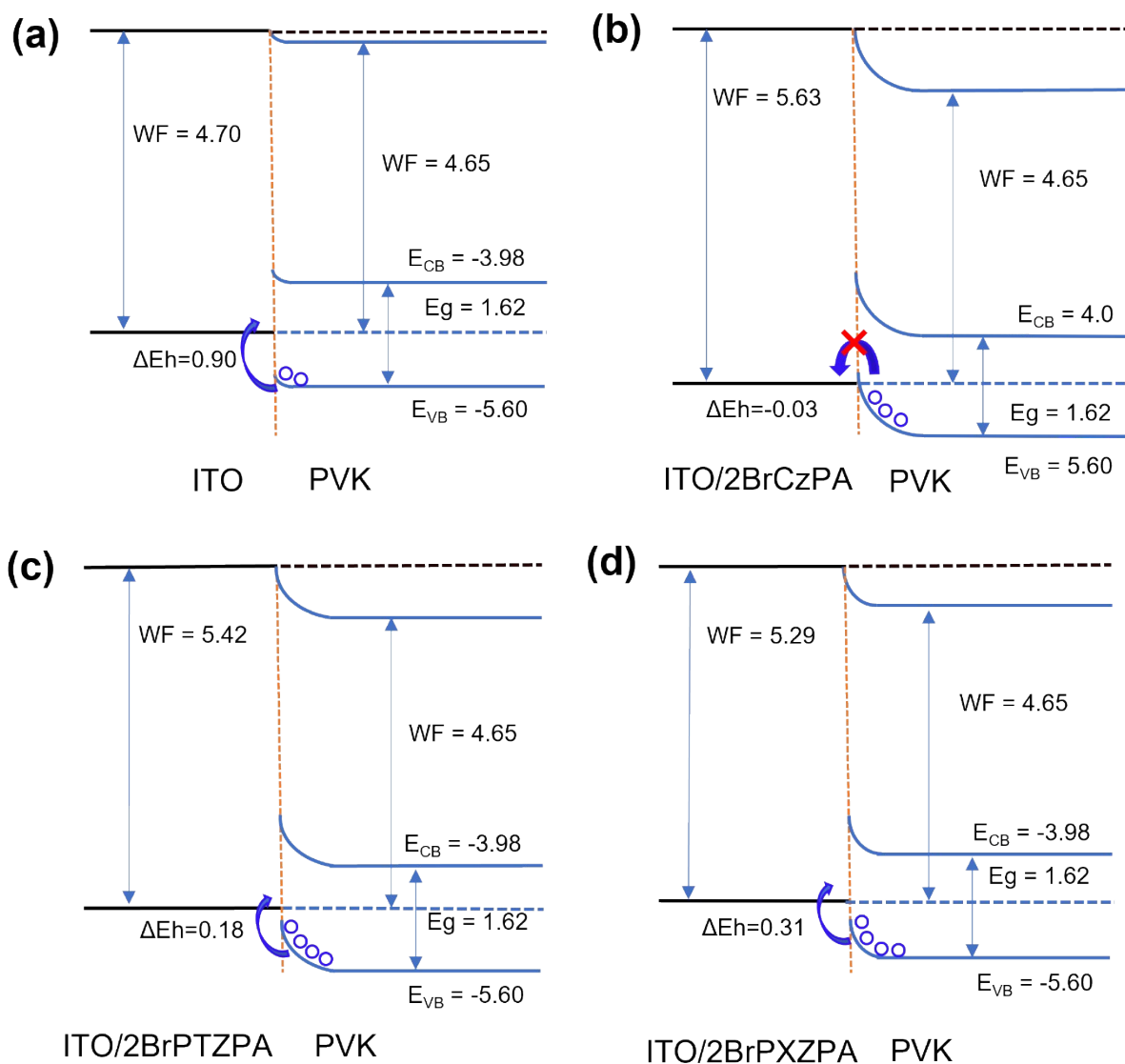


Figure S8 The interface energy level diagram of (a) ITO, (b) ITO/2BrPXZPA, (c) ITO/2BrPTZPA and (d) ITO/2BrPXZPA contact with perovskite.

XPS

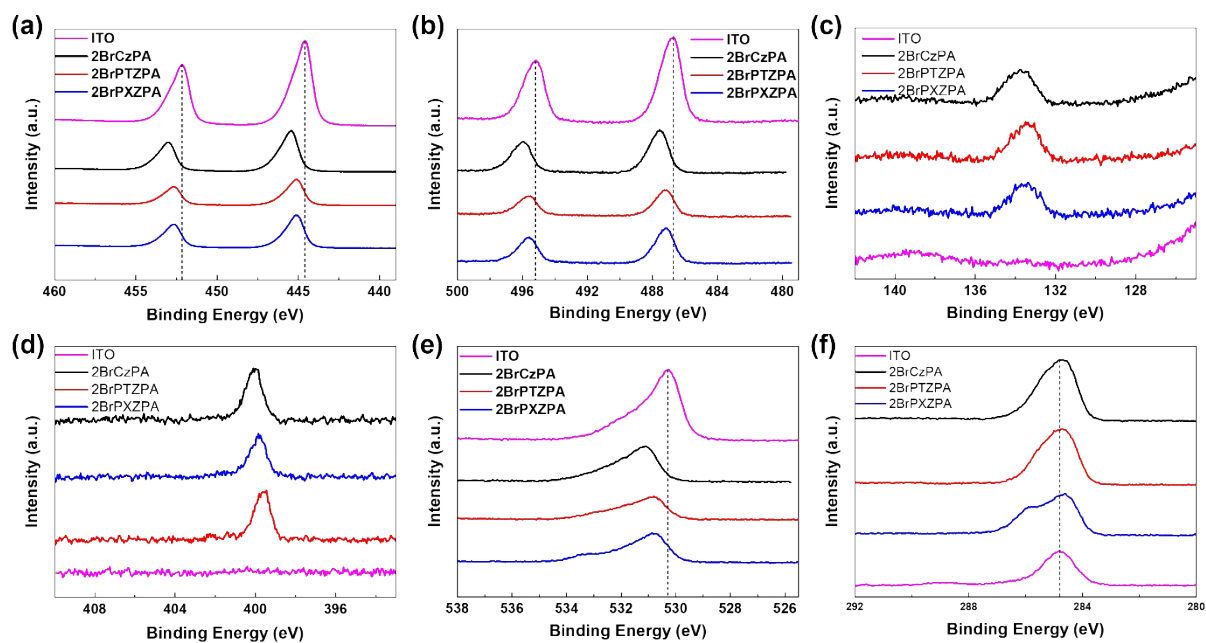


Figure S9 The X-ray photoelectron spectroscopy (XPS) at the (a) In3d, (b) Sn3d, (c) P2p, (d) N1s, (e) O1s, (f) C1s regions of ITO glass with and without SA-HSCs.

Contact angle and surface energy

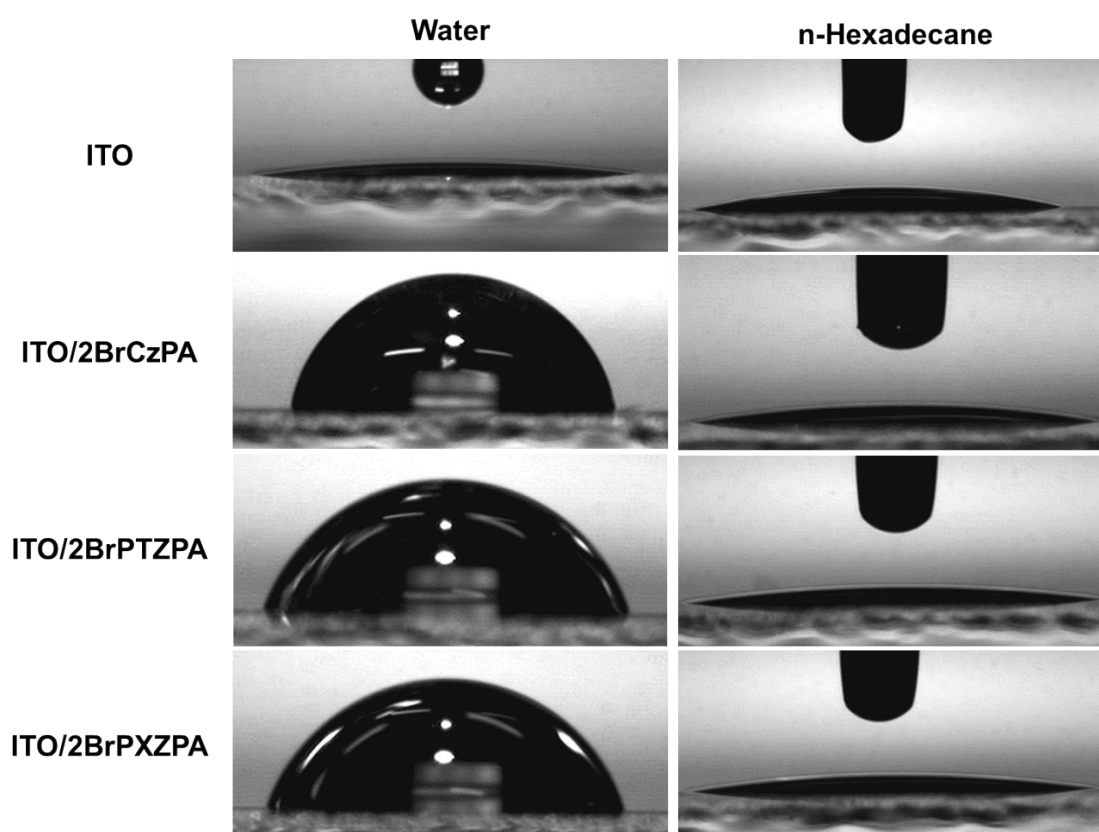


Figure S10 Photographs of water and n-Hexadecane droplets in contact with the various surfaces.

Table S4 Contact angle and surface energy of various surfaces.

| | Water contact angle | n-Hexadecane contact angle | Surface energy (mJ m ⁻²) |
|---------------------|------------------------|-------------------------------|---|
| ITO | 4.43±0.22° | 9.52±0.74° | 73.02 |
| ITO/2BrCzPA | 80.73±1.35° | 7.9±0.74° | 33.59 |
| ITO/2BrPTZPA | 74.20±1.02° | 7.35±0.22° | 36.76 |
| ITO/2BrPXZPA | 72.46±0.90° | 7.52±0.27° | 37.69 |

The surface energy of ITO, 2BrCzPA, 2BrPTZPA and 2BrPXZPA were characterized by two-solution method and calculated with Owens and Wendt equation [3]:

$$(1 + \cos \theta)\gamma_L = 2(\gamma_S^d \gamma_L^d)^{1/2} + 2(\gamma_S^p \gamma_L^p)^{1/2}$$

where γ_S and γ_L are the surface energy of the sample and the probe liquid, respectively. The superscripts d and p refer to the dispersion and polar components of the surface energy, respectively.

SEM

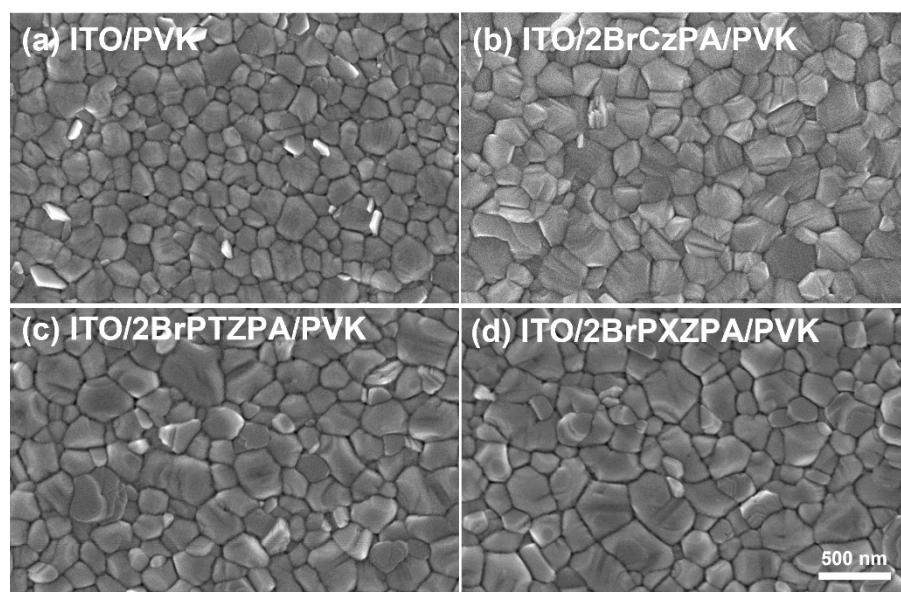


Figure S11 SEM top view of perovskite deposited on (a) ITO, (b) ITO/2BrCzPA, (c) ITO/2BrPTZPA and (d) ITO/2BrPXZPA substrates.

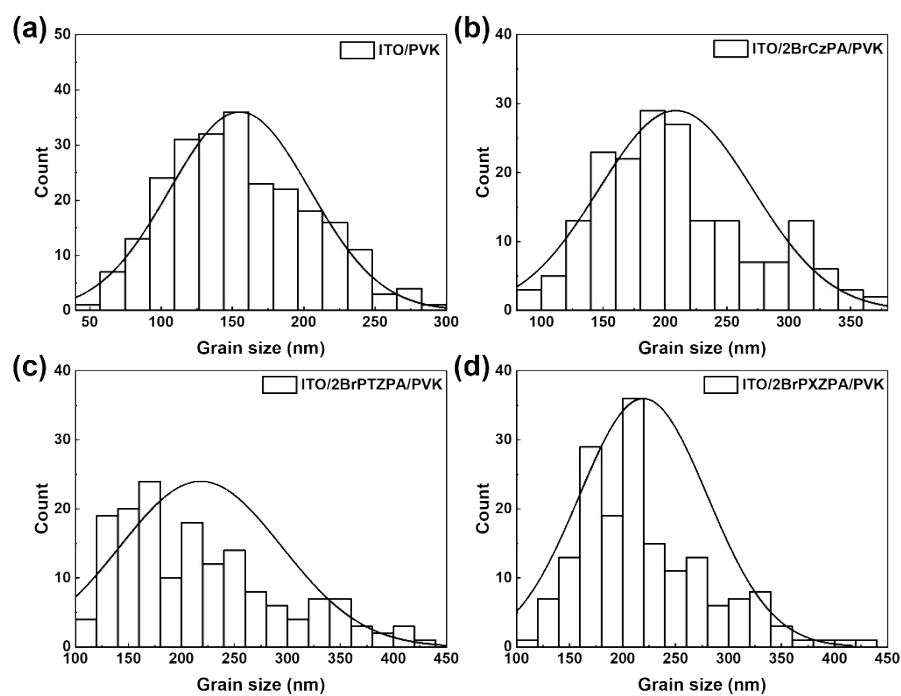


Figure S12 Grain size statistic distribution of perovskite crystals deposited on (a) ITO, (b) ITO/2BrCzPA, (c) ITO/2BrPXZPA and (d) ITO/2BrPTZPA.

Optimization of concentration

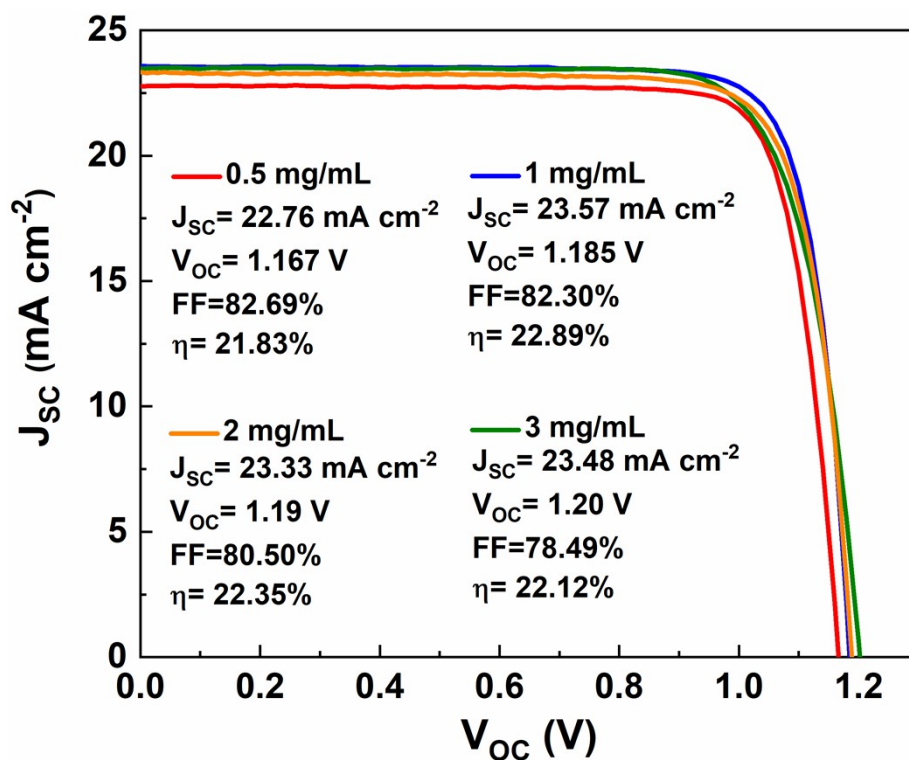


Figure S13 The J-V curves and performance parameters of PSCs based on 2BrPXZPA with different concentration.

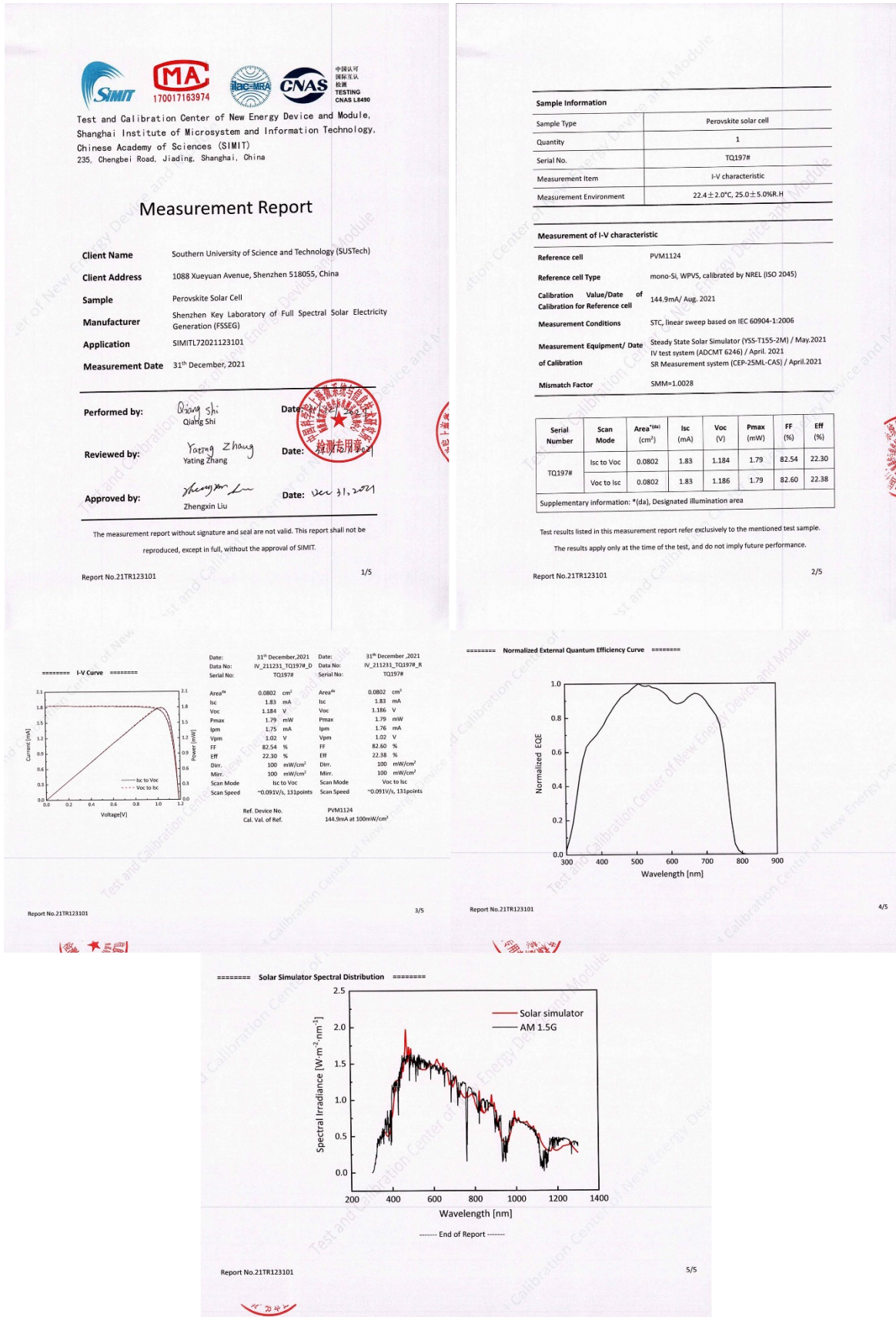


Figure S14 Pictures of certification report for our optimal CsFAMA perovskite solar cell device with 2BrPXZPA in the certification centre of the New Energy Device and Module at Shanghai Institute of Microsystem and Information Technology (SIMIT), China.

PTAA-based device performance

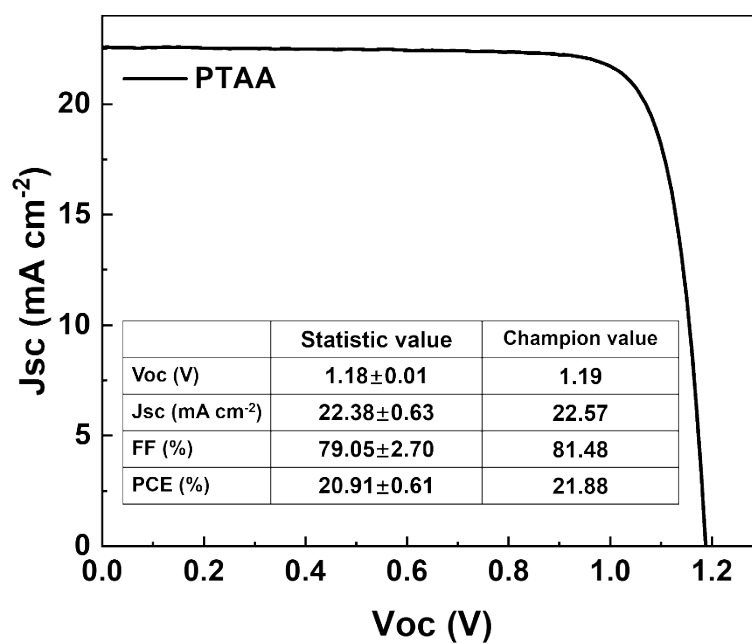


Figure S15 The J-V curve of PTAA-based PSCs, and the statistic parameters were got from 12 devices.

Table S5 Fitted results of the TRPL spectra of perovskite film deposited on glass, 2BrPTZPA and 2BrPXZPA substrates.

| | A₁ | τ₁ (ns) | A₂ | τ₂ (ns) | τ_{ave} (ns) |
|-----------------|----------------------|---------------------------|----------------------|---------------------------|-----------------------------|
| Glass | 0.973 | 0.51 | 0.017 | 39.41 | 22.86 |
| 2BrCzPA | 0.523 | 5.27 | 0.376 | 118.61 | 112.01 |
| 2BrPTZPA | 0.534 | 5.76 | 0.337 | 145.96 | 137.71 |
| 2BrPXZPA | 0.434 | 0.08 | 0.440 | 168.86 | 168.78 |

The TRPL decay spectra were fitted by a biexponential function:

$$y = y_0 + A_1 e^{-x/\tau_1} + A_2 e^{-x/\tau_2}$$

and the average decay lifetime was calculated with function:

$$\tau_{average} = \frac{A_1 \tau_1^2 + A_2 \tau_2^2}{A_1 \tau_1 + A_2 \tau_2}$$

ECM and fitting results for EIS

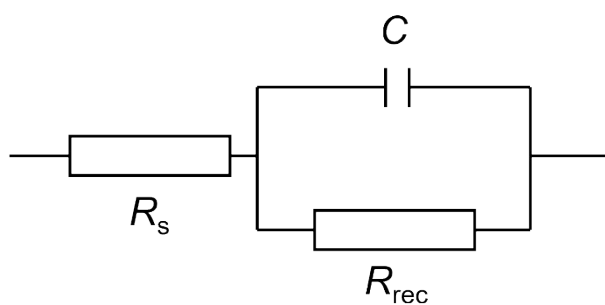


Figure S16 The equivalent-circuit model (ECM) employed for EIS fitting of PSC devices.

Table S6 EIS parameters for the PSCs based on various SA-HSMs.

| SA-HEMs | R_s (Ω) | R_{rec} (Ω) |
|----------|--------------------|------------------------|
| 2BrCzPA | 7.9 | 2029 |
| 2BrPTZPA | 13.3 | 2906 |
| 2BrPXZPA | 12.5 | 3112 |

NMR and HRMS spectra

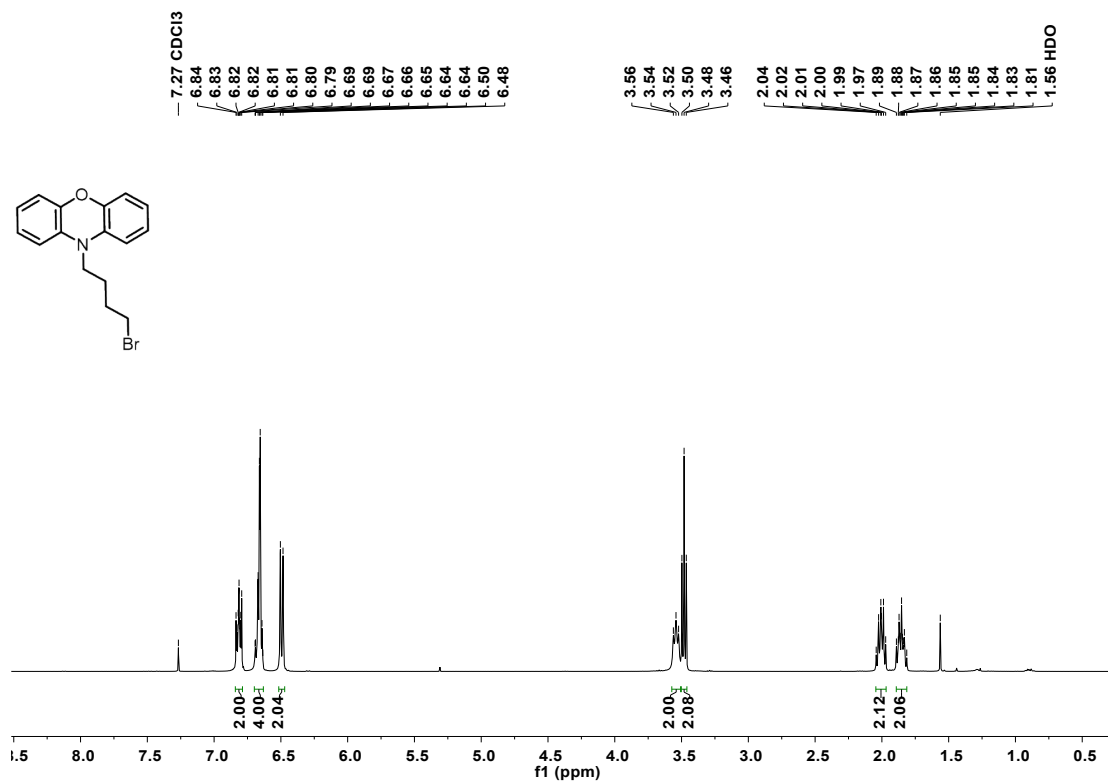


Figure S17 ¹H NMR spectrum of PXZC4Br.

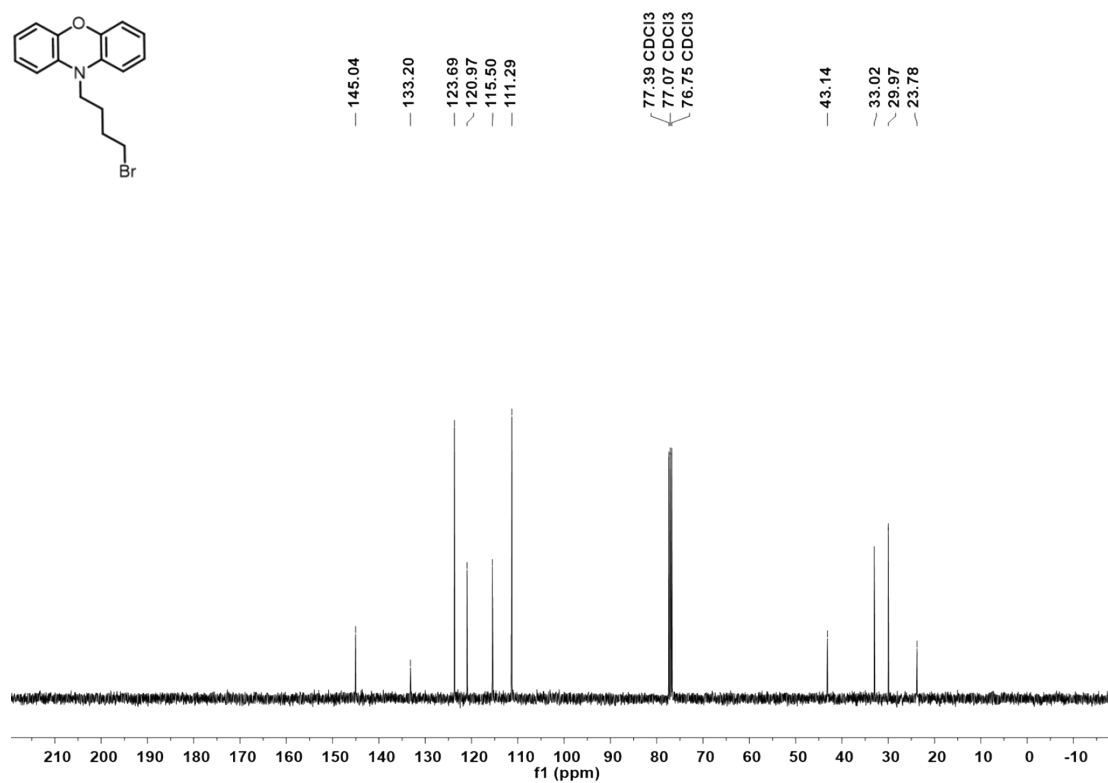


Figure S18 ¹³C NMR spectrum of PXZC4Br.

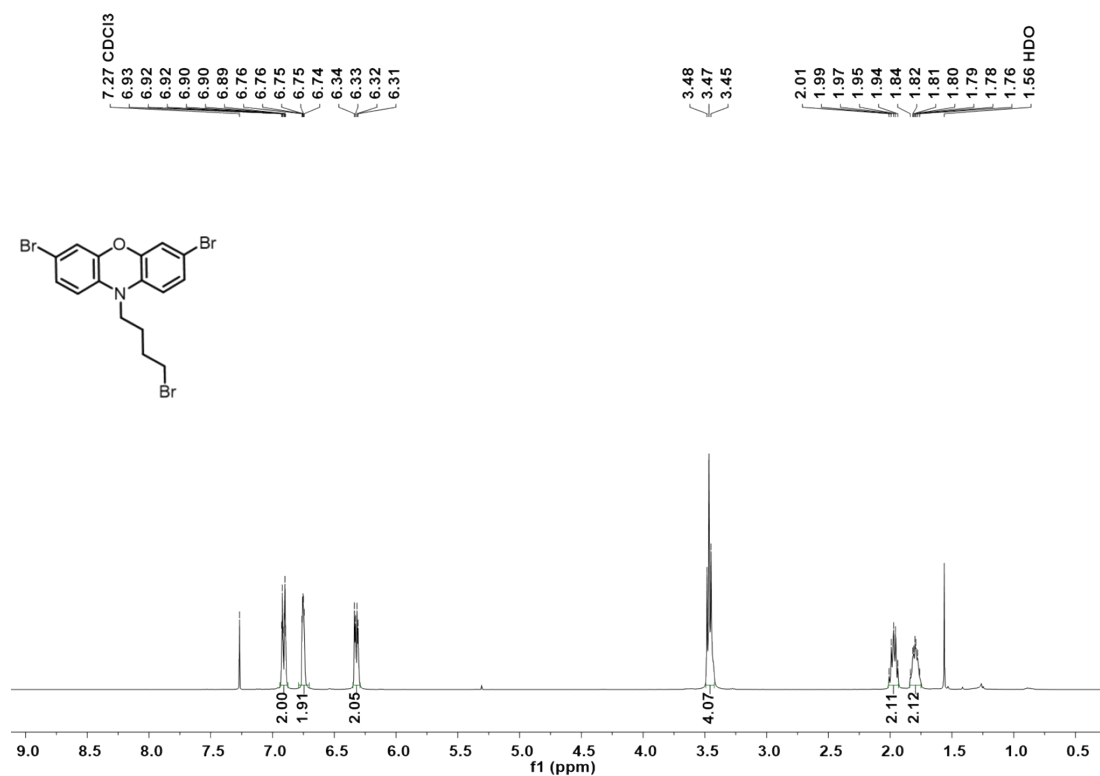


Figure S19 ¹H NMR spectrum of 2BrPXZC4Br.

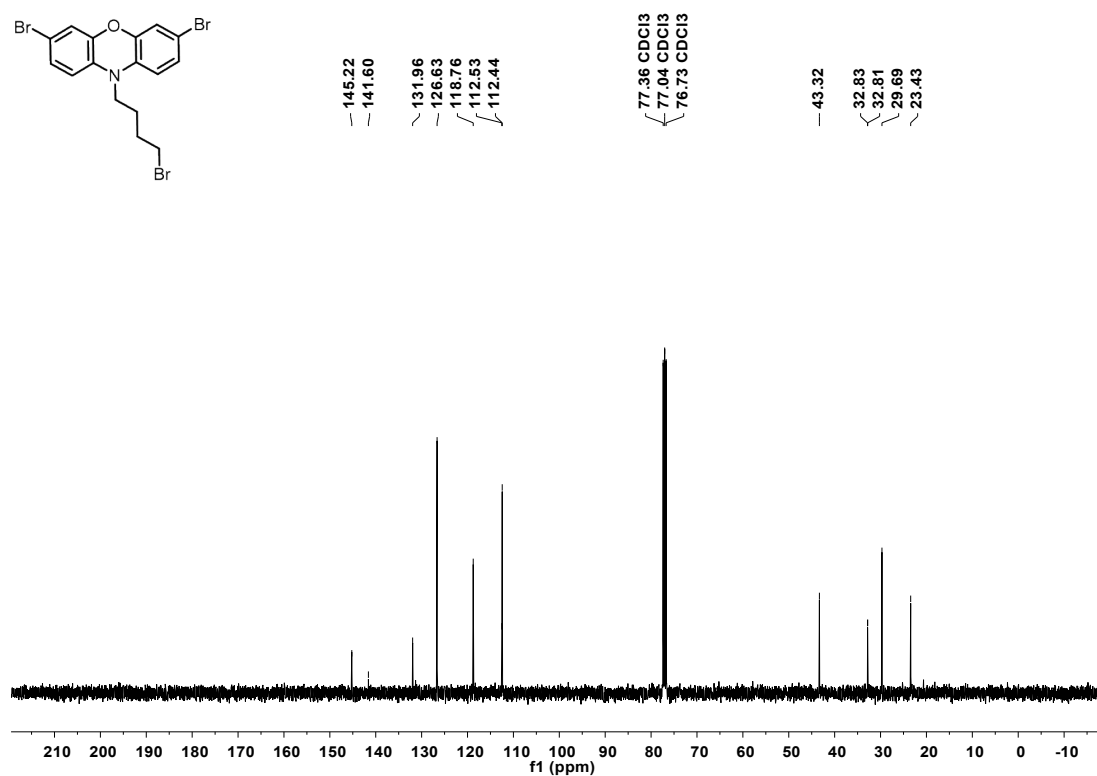


Figure S20 ¹³C NMR spectrum of 2BrPXZC4Br.

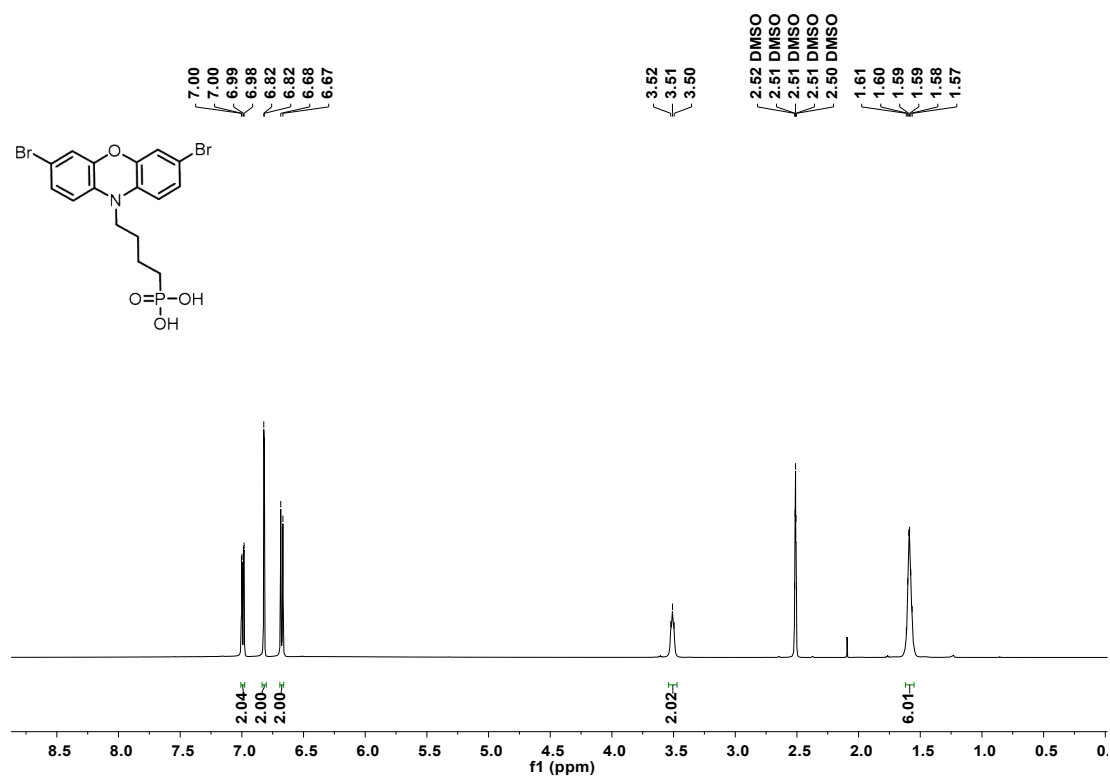


Figure S21 ¹H NMR spectrum of 2BrPXZPA.

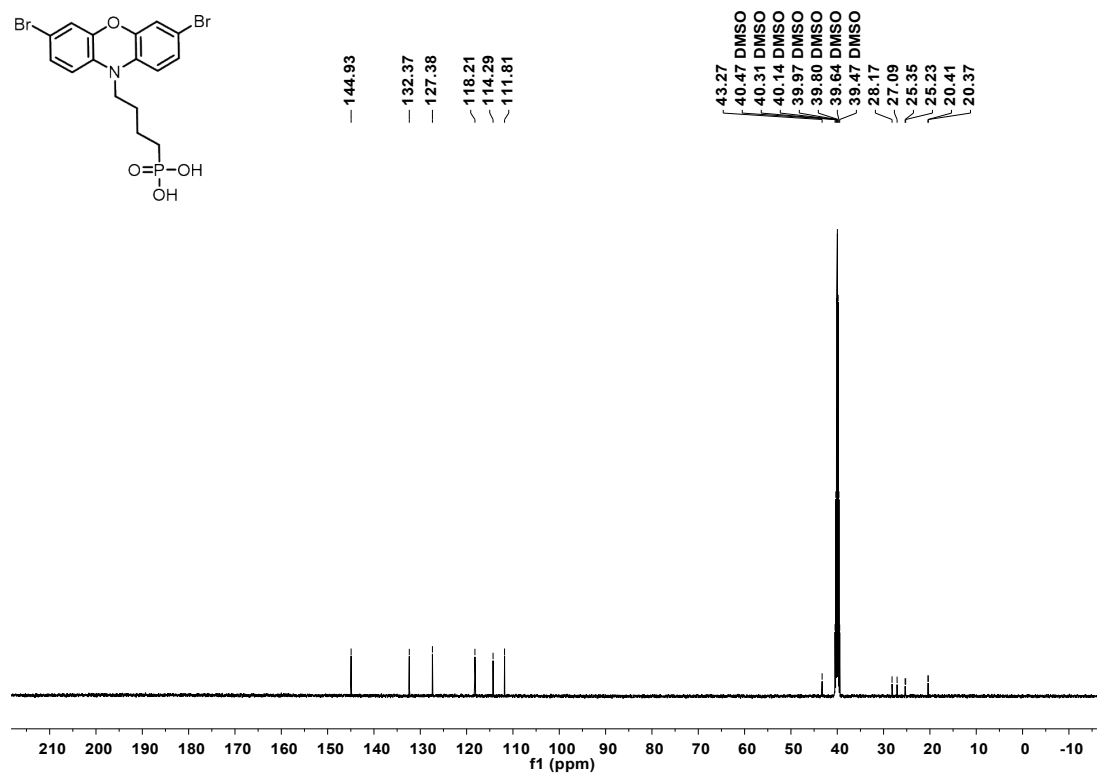


Figure S22 ¹³C NMR spectrum of 2BrPXZPA.

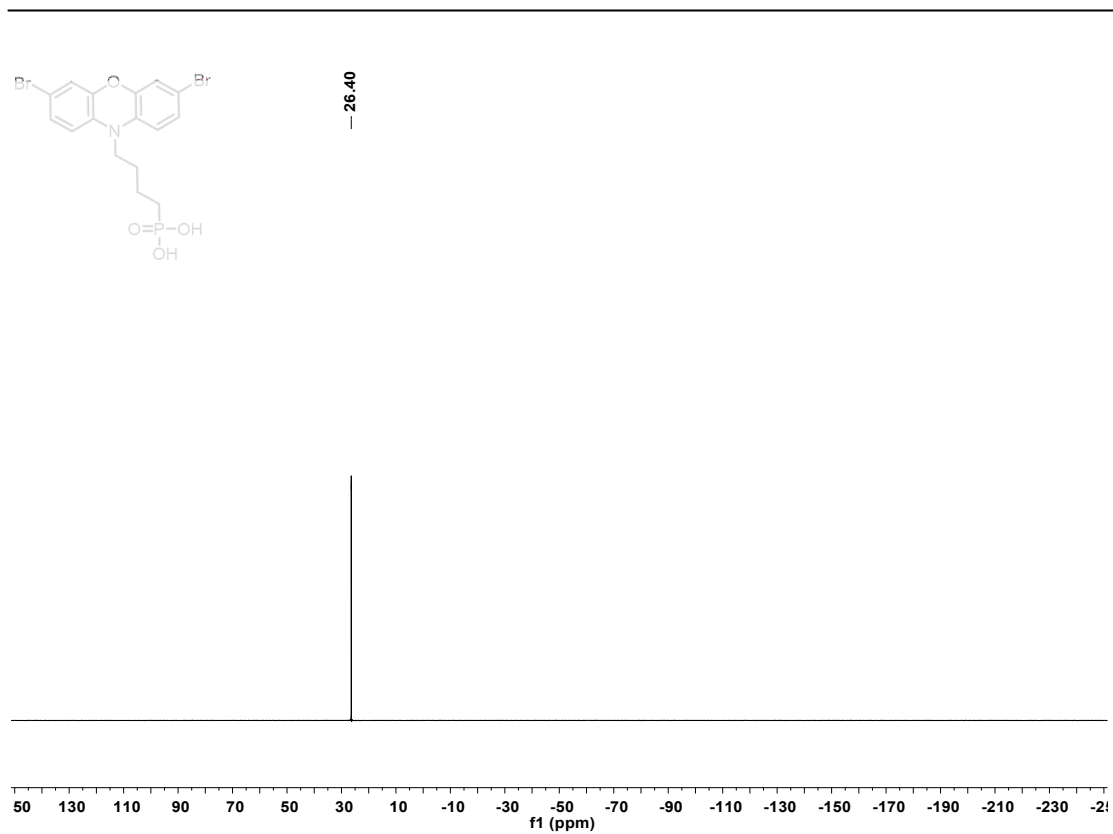


Figure S23 ^{31}P NMR spectrum of 2BrPXZPA.

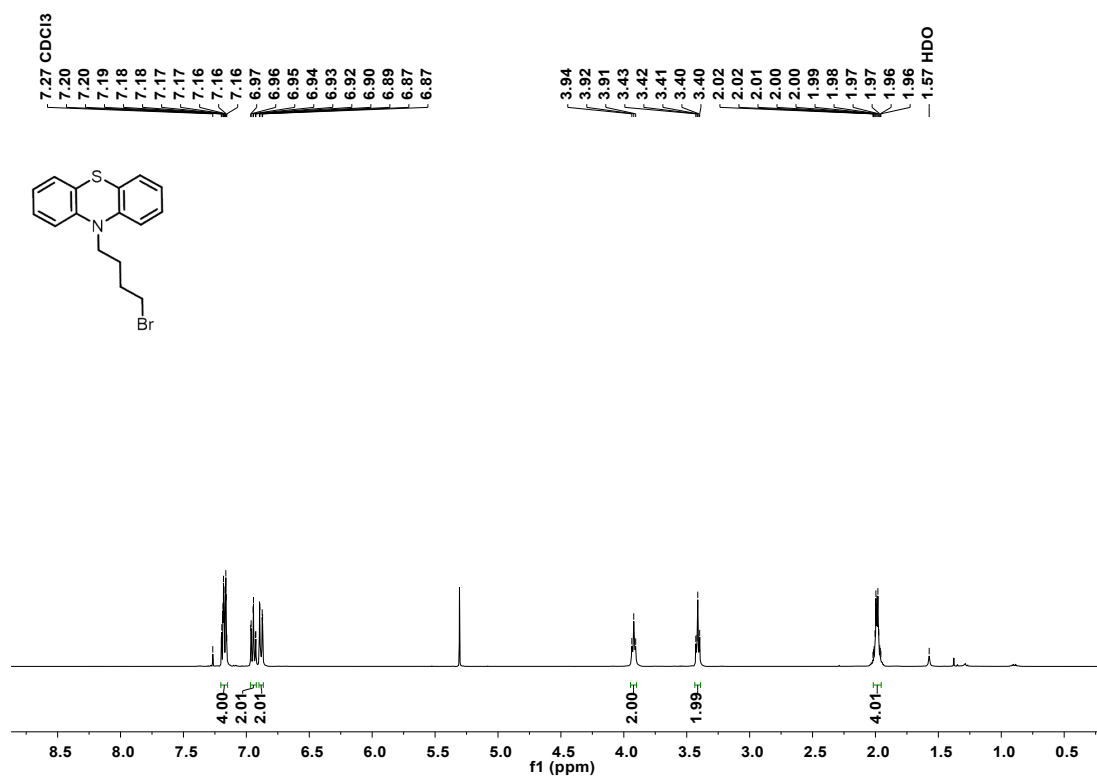


Figure S24 ^1H NMR spectrum of PTZC4Br.

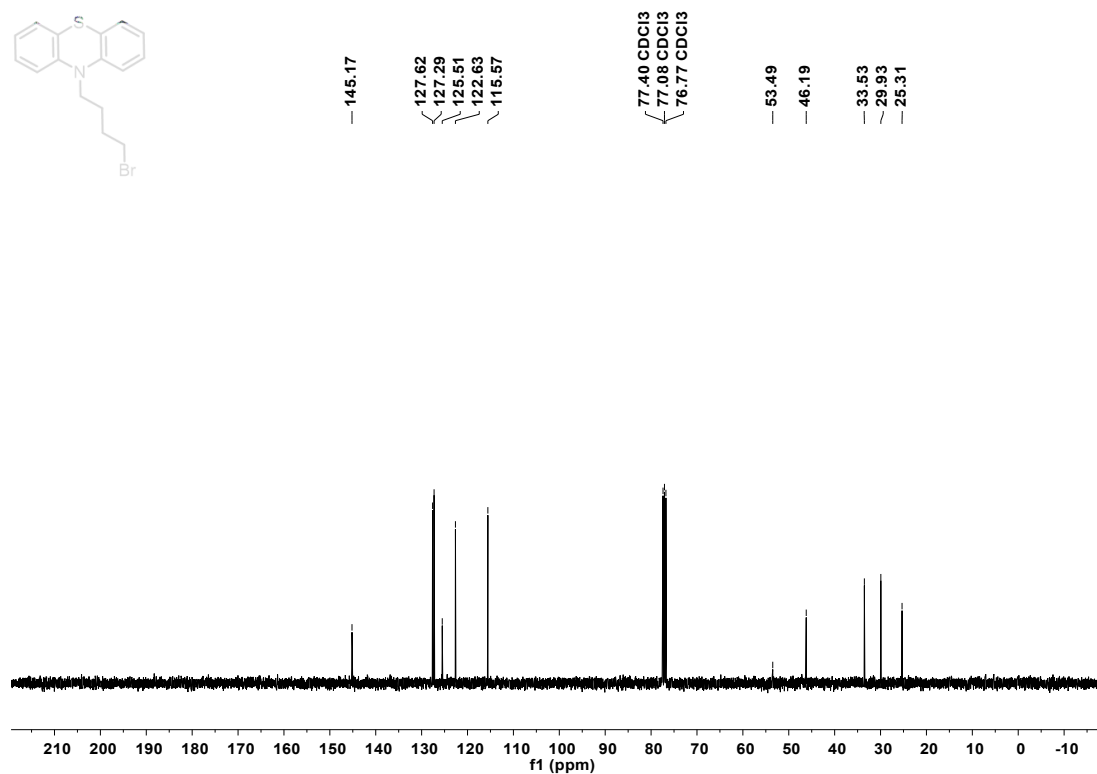


Figure S25 ^{13}C NMR spectrum of PTZC4Br.

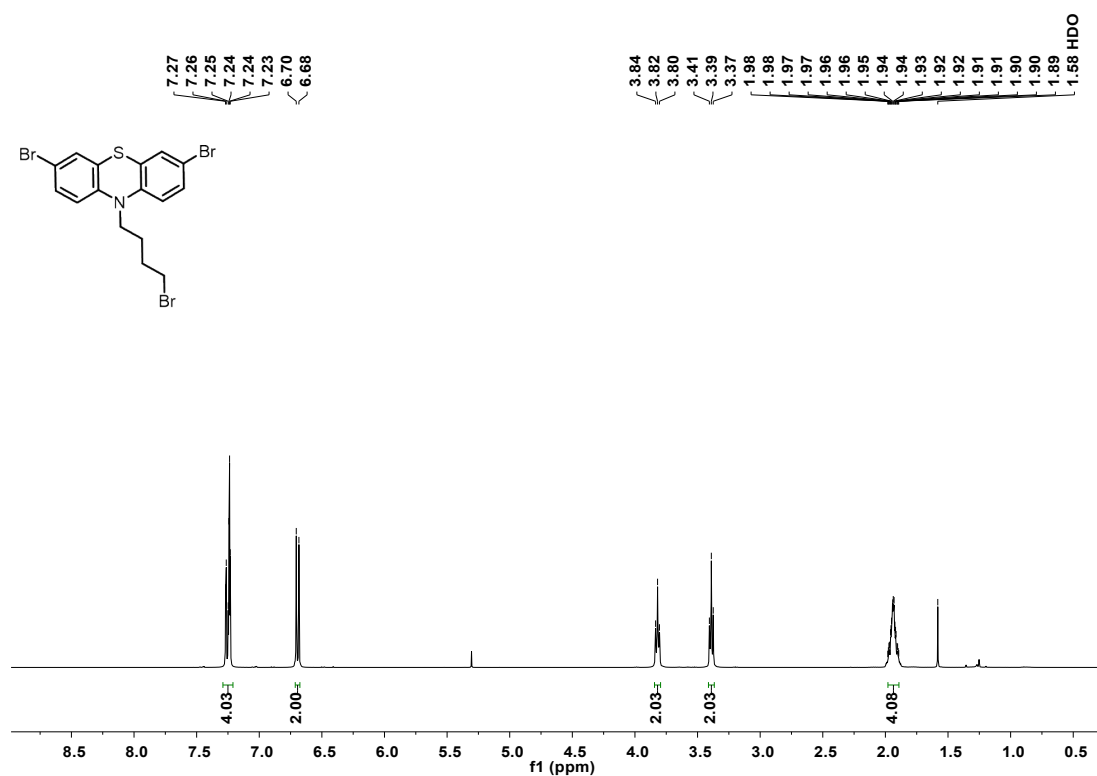


Figure S26 ^1H NMR spectrum of 2BrPTZC4Br.

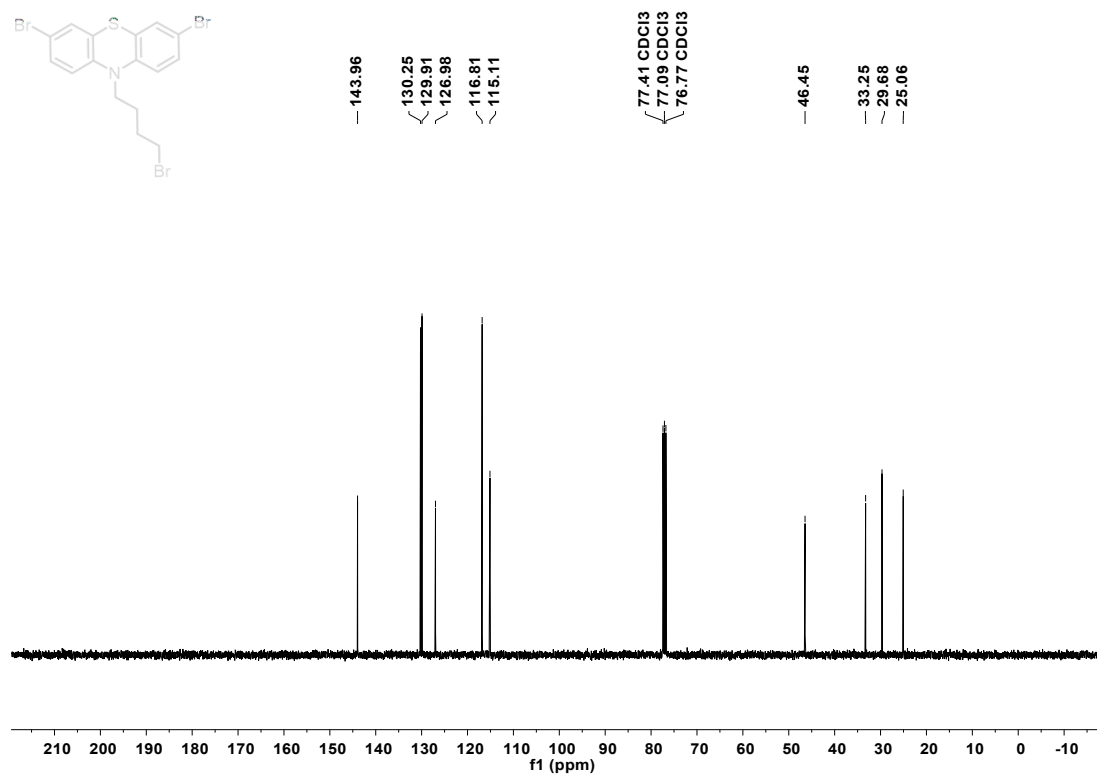


Figure S27 ^{13}C NMR spectrum of 2BrPTZC4Br.

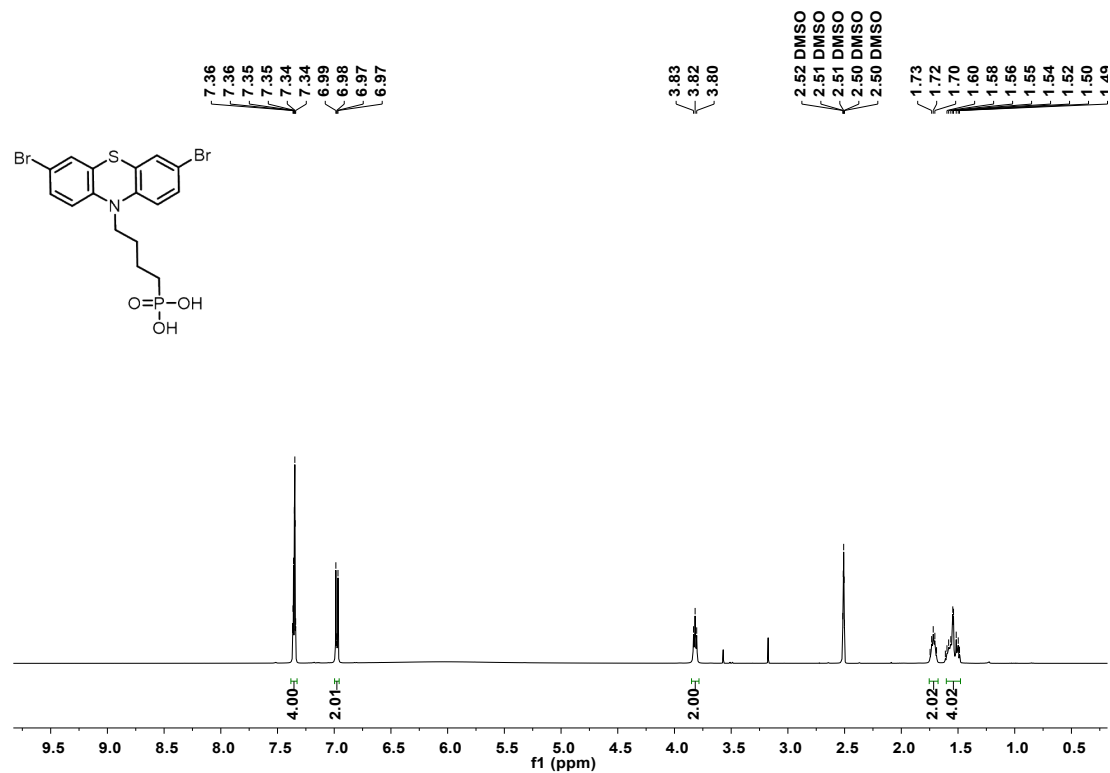


Figure S28 ^1H NMR spectrum of 2BrPTZPA.

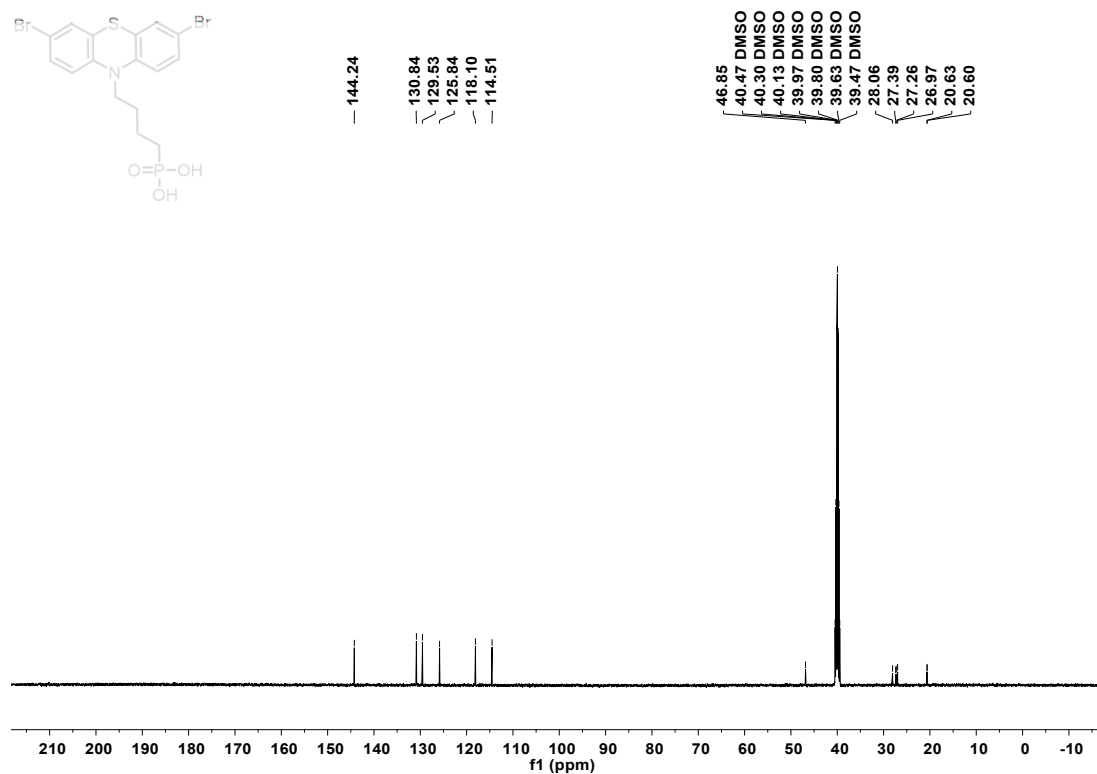


Figure S29 ^{13}C NMR spectrum of 2BrPTZPA.

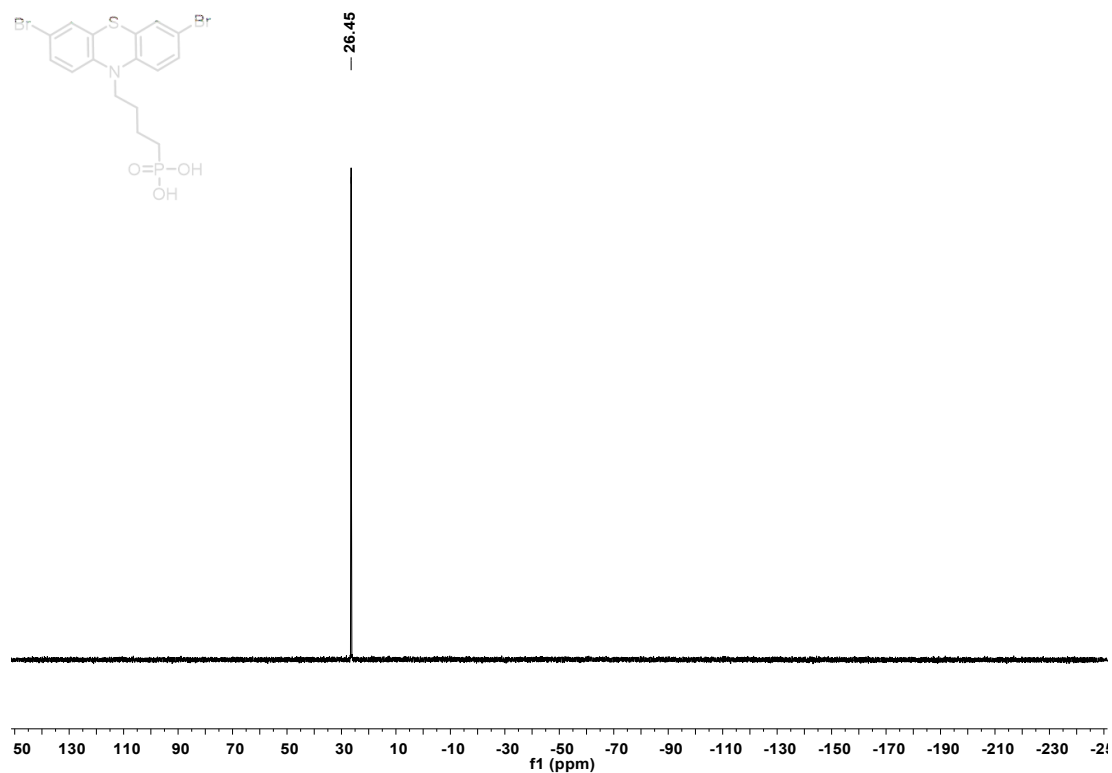


Figure S30 ^{31}P NMR spectrum of 2BrPTZPA.

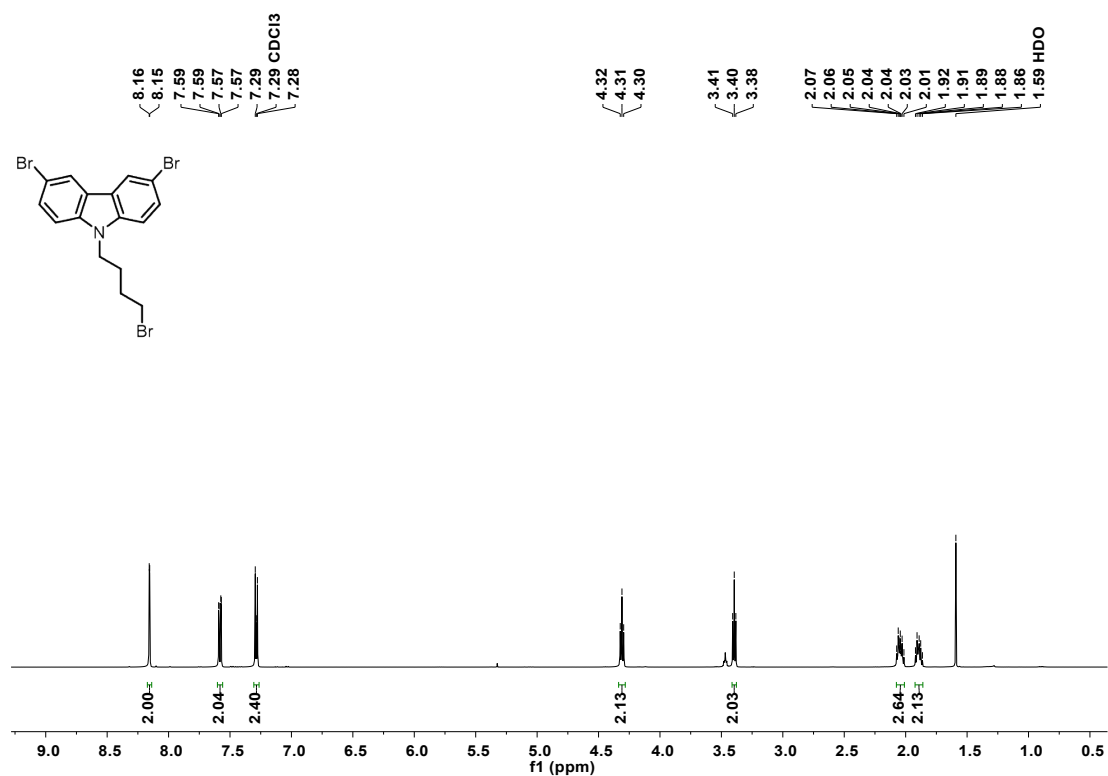


Figure S31 ¹H NMR spectrum of 2BrCzC4Br.

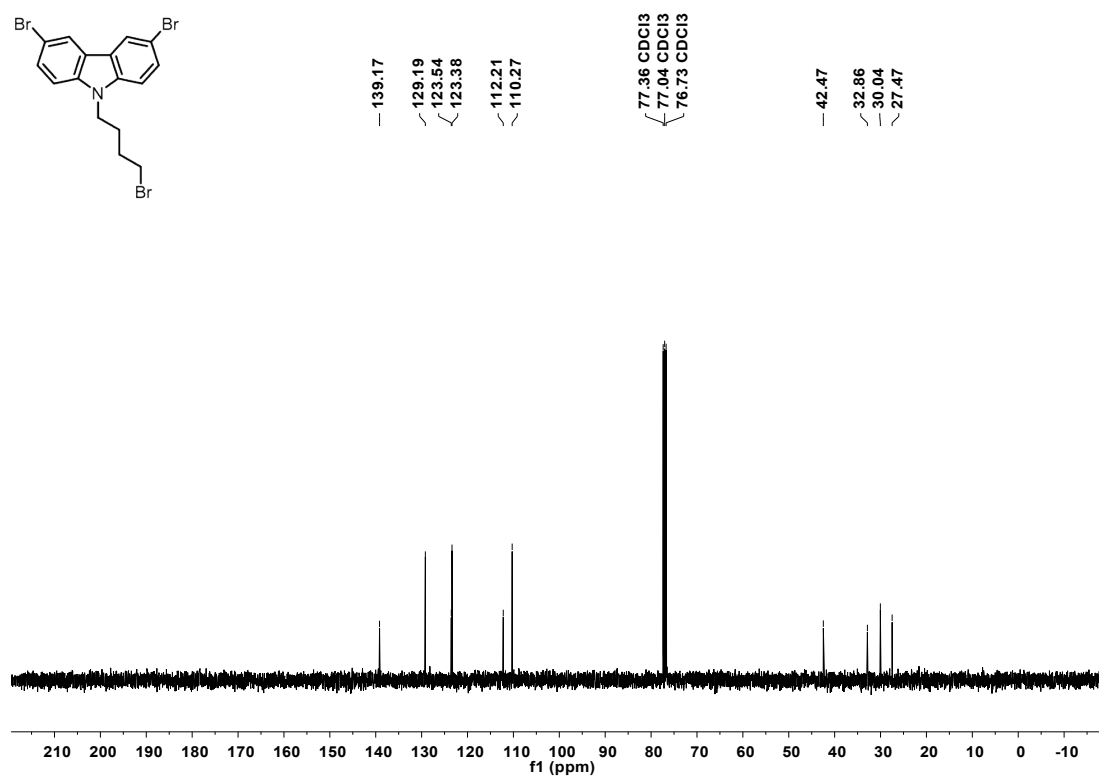


Figure S32 ¹³C NMR spectrum of 2BrCzC4Br.

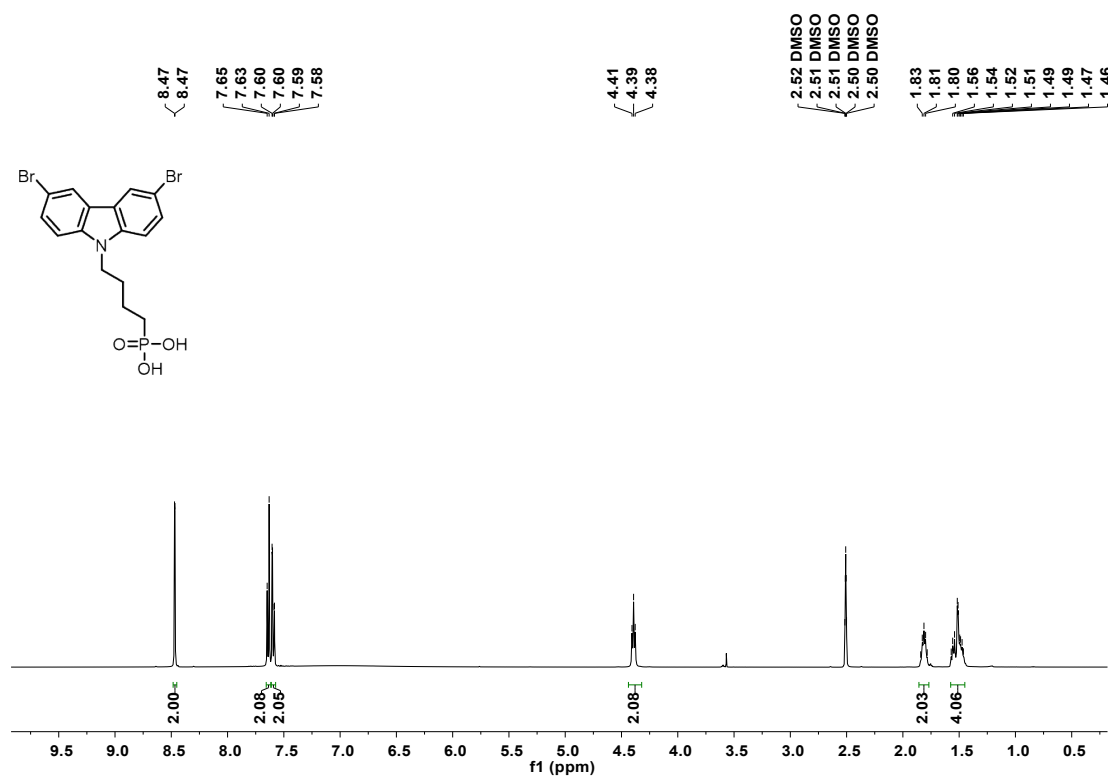


Figure S33 ^1H NMR spectrum of 2BrCzPA.

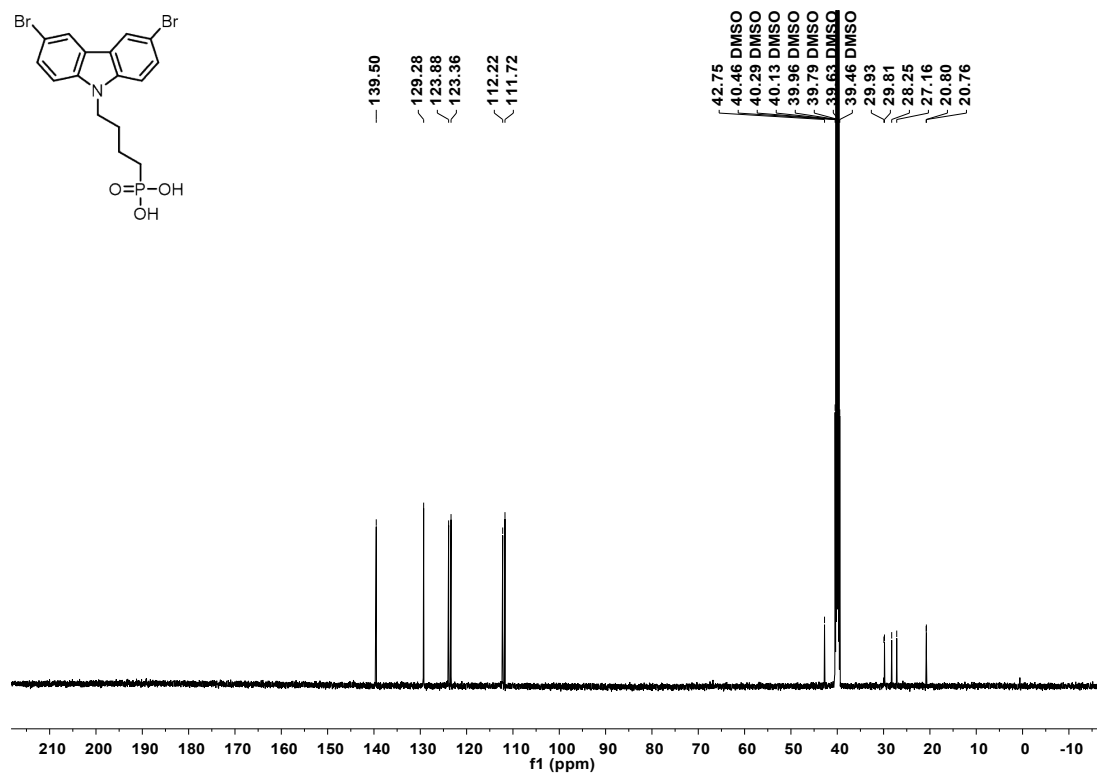


Figure S34 ^{13}C NMR spectrum of 2BrCzPA.

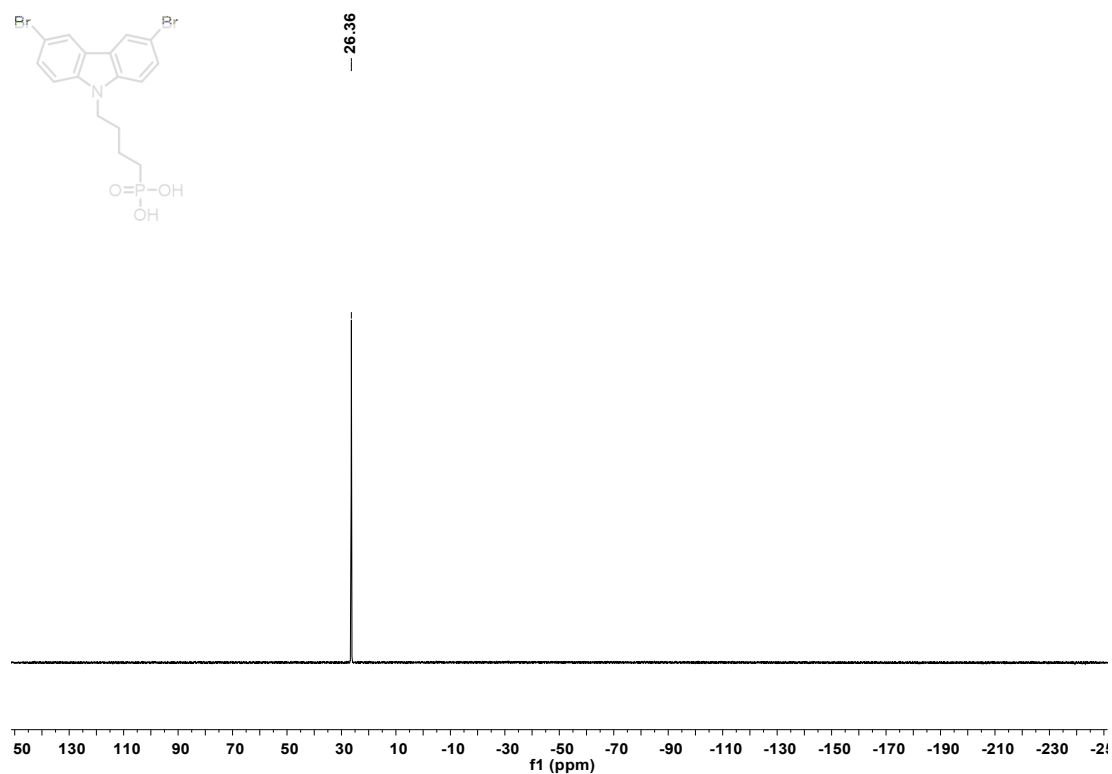


Figure S35 ^{31}P NMR spectrum of 2BrCzPA.

ZOOM IN, $[\text{M}+\text{H}]^+$

3 20211223150805 #18-23 RT: 0.19-0.23 AV: 3 NL: 3.10E8
T: FTMS + p ESI Full ms [200.0000-1000.0000]

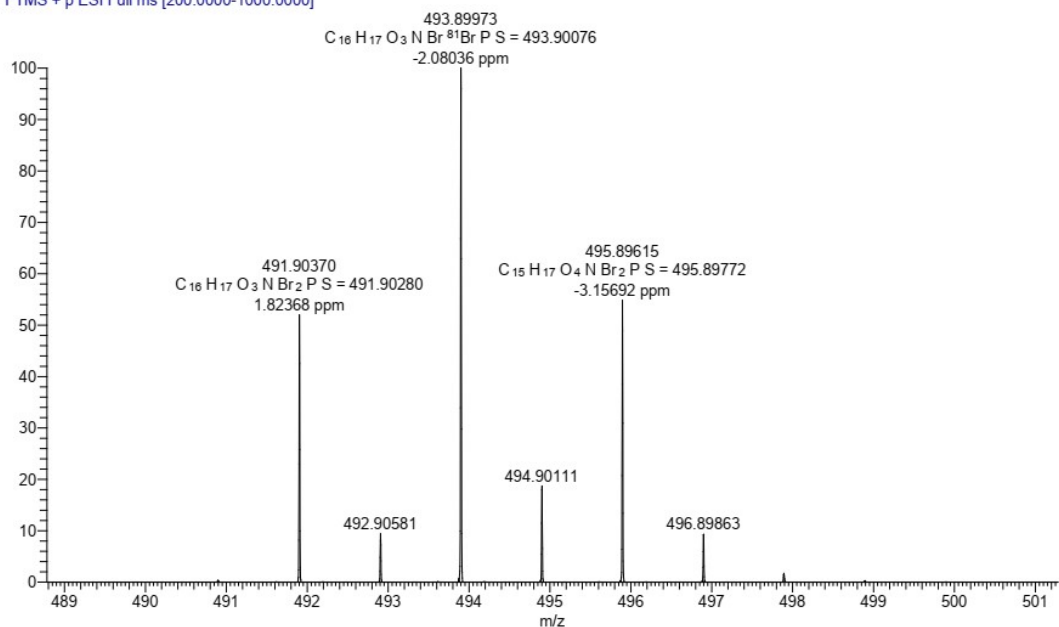


Figure S36 HRMS spectrum of 2BrPTZPA.

ZOOM IN, [M+H]⁺

2_20211223150538 #18-30 RT: 0.19-0.29 AV: 6 NL: 3.19E8
T: FTMS + p ESI Full ms [200.0000-1000.0000]

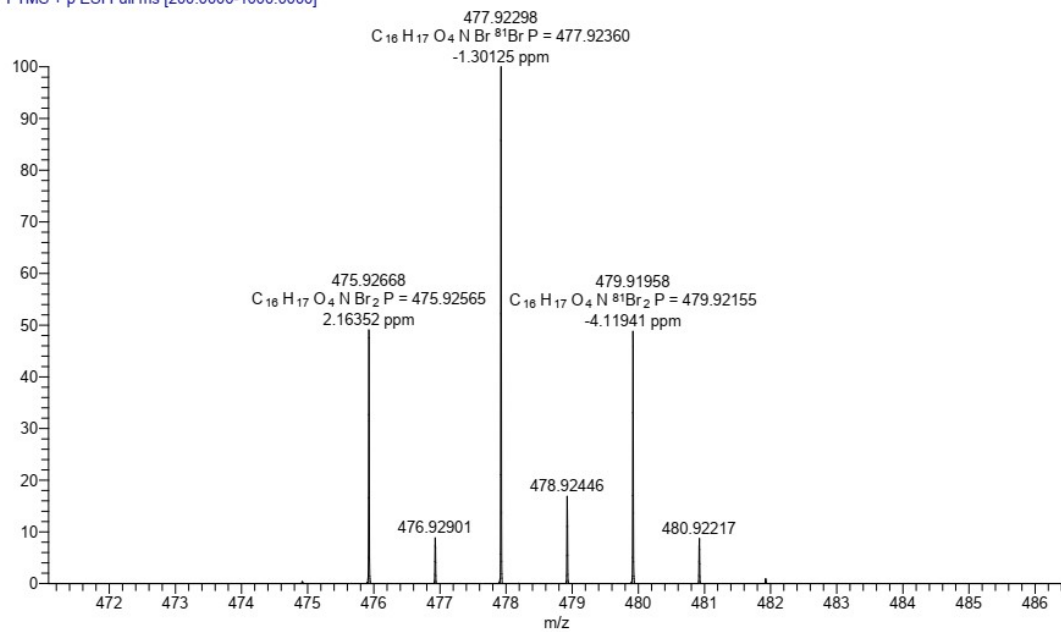


Figure S37 HRMS spectrum of 2BrPXZPA.

ZOOM IN, [M+H]⁺

1_20211223150205 #17-26 RT: 0.17-0.25 AV: 5 NL: 2.93E8
T: FTMS + p ESI Full ms [200.0000-1000.0000]

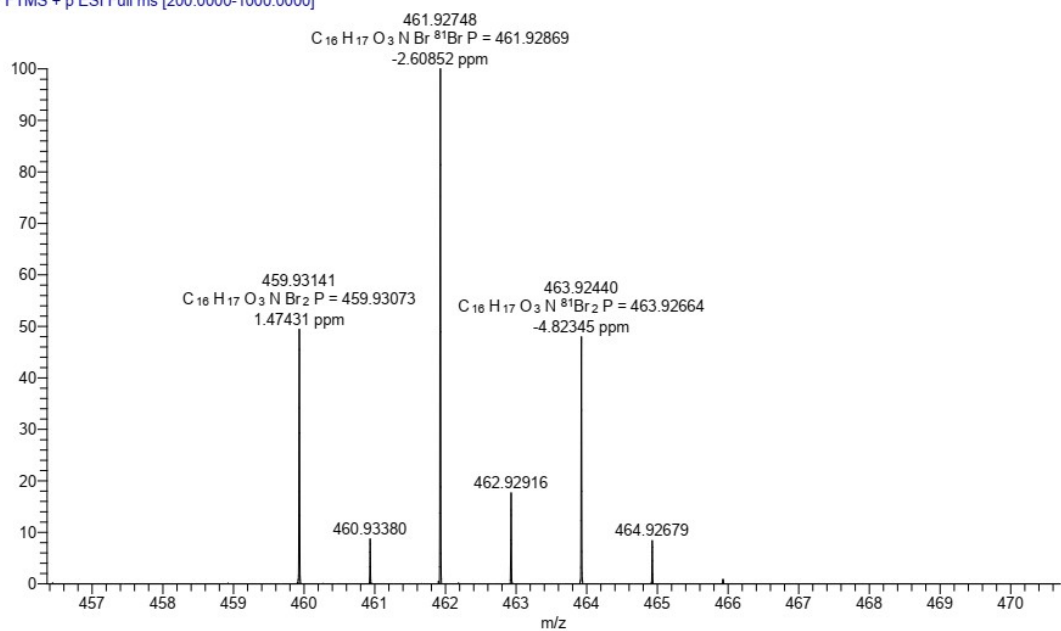


Figure S38 HRMS spectrum of 2BrCzPA.

Reference

- [1] Gaussian 09, Revision D.01, M. J. Frisch, G. W. Trucks, H. B. Schlegel, G. E. Scuseria, M. A. Robb, J. R. Cheeseman, G. Scalmani, V. Barone, B. Mennucci, G. A. Petersson, H. Nakatsuji, M. Caricato, X. Li, H. P. Hratchian, A. F. Izmaylov, J. Bloino, G. Zheng, J. L. Sonnenberg, M. Hada, M. Ehara, K. Toyota, R. Fukuda, J. Hasegawa, M. Ishida, T. Nakajima, Y. Honda, O. Kitao, H. Nakai, T. Vreven, J. A. Montgomery, Jr., J. E. Peralta, F. Ogliaro, M. Bearpark, J. J. Heyd, E. Brothers, K. N. Kudin, V. N. Staroverov, T. Keith, R. Kobayashi, J. Normand, K. Raghavachari, A. Rendell, J. C. Burant, S. S. Iyengar, J. Tomasi, M. Cossi, N. Rega, J. M. Millam, M. Klene, J. E. Knox, J. B. Cross, V. Bakken, C. Adamo, J. Jaramillo, R. Gomperts, R. E. Stratmann, O. Yazyev, A. J. Austin, R. Cammi, C. Pomelli, J. W. Ochterski, R. L. Martin, K. Morokuma, V. G. Zakrzewski, G. A. Voth, P. Salvador, J. J. Dannenberg, S. Dapprich, A. D. Daniels, O. Farkas, J. B. Foresman, J. V. Ortiz, J. Cioslowski, and D. J. Fox, Gaussian, Inc., Wallingford CT, 2013.
- [2] Al-Ashouri, A.; Magomedov, A.; Roß, M.; Jošt, M.; Talaikis, M.; Chistiakova, G.; Bertram, T.; Márquez, J. A.; Köhnen, E.; Kasparavičius, E.; Levcenco, S.; Gil-Escrig, L.; Hages, C. J.; Schlattmann, R.; Rech, B.; Malinauskas, T.; Unold, T.; Kaufmann, C. A.; Korte, L.; Niaura, G.; Getautis, V.; Albrecht, S., Conformal monolayer contacts with lossless interfaces for perovskite single junction and monolithic tandem solar cells. *Energy Environ. Sci.* 2019, 12 (11), 3356-3369.
- [3] Chen, X.; Zhang, Z.; Ding, Z.; Liu, J.; Wang, L., Diketopyrrolopyrrole-based Conjugated Polymers Bearing Branched Oligo(Ethylene Glycol) Side Chains for Photovoltaic Devices. *Angew. Chem. Int. Ed.* 2016, 55 (35), 10376-10380.